

## Study of the Level Structure of $N = 82$ Nuclei via Proton-Transfer Reactions\*

B. H. Wildenthal†

*Michigan State University, East Lansing, Michigan ‡ 48823  
and Oak Ridge National Laboratory, Oak Ridge, Tennessee 37830*

and

E. Newman and R. L. Auble

*Oak Ridge National Laboratory, Oak Ridge, Tennessee 37830*

(Received 19 June 1970)

Measurements of the angular distributions of the ( $^3\text{He}, d$ ) and ( $d, ^3\text{He}$ ) reactions on the stable, even-mass  $N = 82$  isotones are presented and discussed. In each of the residual nuclei formed in these reactions,  $^{135}\text{I}$ ,  $^{137}\text{Cs}$ ,  $^{139}\text{La}$ ,  $^{141}\text{Pr}$ ,  $^{143}\text{Pm}$ , and  $^{145}\text{Eu}$ , the lowest two levels are populated with significant strength, one by  $l_p = 4$  transfer and one by  $l_p = 2$  transfer. Analysis indicates that these states result from coupling a  $1g_{7/2}$  or  $2d_{5/2}$  proton (or proton hole) to the respective  $J^\pi = 0^+$  target ground states. The relative energies of these states change as a function of mass, the  $\frac{3}{2}^+$  state lying 590 keV above the  $\frac{1}{2}^+$  state in  $^{135}\text{I}$ , and 330 keV below the  $\frac{1}{2}^+$  state in  $^{145}\text{Eu}$ . Spectroscopic factors extracted from the data with distorted-wave Born-approximation analysis indicate that the active particles in the target ground states predominantly occupy the  $1g_{7/2}$  and  $2d_{5/2}$  orbits, with the ratio of  $1g_{7/2}$  protons to  $2d_{5/2}$  protons varying from 3.5/0.5 for  $^{136}\text{Xe}$  to 6.3/3.6 for  $^{144}\text{Sm}$ . The pickup reactions reveal small admixtures of  $1h_{11/2}$ ,  $3s_{1/2}$ , and  $2d_{3/2}$  protons into the heavier target ground states. These orbits, together with the  $1g_{7/2}$  and  $2d_{5/2}$ , constitute the major shell which fills between  $Z = 50$  and 82. The stripping experiments locate the centroid energies of these higher three orbits relative to the  $\frac{5}{2}^+$  and  $\frac{1}{2}^+$  states. It is found that the centroids of the  $1h_{11/2}$ ,  $3s_{1/2}$ , and  $2d_{3/2}$  single-particle states relative to the ground states decrease monotonically from excitations of 1.9, 2.1, and 2.1 MeV, respectively, in  $^{137}\text{Cs}$  to excitations of 0.72, 0.81, and 1.1 MeV in  $^{145}\text{Eu}$ .

### I. INTRODUCTION

This paper reports the results of a comprehensive experimental study<sup>1-3</sup> of the low-energy level structure ( $\leq 3$  MeV) of odd-mass nuclei which have a neutron number of 82. The data to be discussed consist of the spectra of the ( $d, ^3\text{He}$ ) and ( $^3\text{He}, d$ ) reactions on  $^{136}\text{Xe}$ ,  $^{138}\text{Ba}$ ,  $^{140}\text{Ce}$ ,  $^{142}\text{Nd}$ , and  $^{144}\text{Sm}$ . From these spectra, energy levels are located in the residual nuclei  $^{135}\text{I}$ ,  $^{137}\text{Cs}$ ,  $^{139}\text{La}$ ,  $^{141}\text{Pr}$ ,  $^{143}\text{Pm}$ , and  $^{145}\text{Eu}$ . The measurements of the differential cross sections of the transitions to these levels are analyzed with the distorted-wave Born-approximation (DWBA) theory in order to extract the values of the orbital angular momenta ( $l_p$ ) of the protons transferred between the target and final states. From this information, the parities of the various final states are determined, and limits ( $J = l_p \pm \frac{1}{2}$ ) placed on their spins. In addition, and of comparable importance, the DWBA analysis of the angular distributions yields the intrinsic strengths [spectroscopic factors  $S(nl j)$ ] of the various transitions. These strengths, which correspond to the expectation values of appropriate single-particle creation or annihilation operators between the initial and final states, relate the structure of the residual states to that of the tar-

get ground state. They also provide information about the occupation probabilities of the shell-model orbits which are actively involved in the structure of the low-lying energy levels.

The purpose of these experiments has been to obtain quantitative experimental information necessary for the initiation and evaluation of detailed theoretical studies of nuclear structure in this region. The most general tenets of the nuclear shell model<sup>4</sup> indicate that systems of 50 and 82 nucleons each constitute unusually tightly bound (and hence stable) aggregates. In this formulation the nucleons which are added as the proton or neutron number is increased from 51 to 82 occupy single-particle orbits in the average shell-model potential which are characterized by the quantum numbers  $1g_{7/2}$ ,  $2d_{5/2}$ ,  $2d_{3/2}$ ,  $3s_{1/2}$ , and  $1h_{11/2}$ . We shall in the future refer to these orbits as constituting the "gdhs" major shell. In the present experiments we are dealing with nuclei which have 82 neutrons and from 53 to 63 protons. The chart of the nuclides in this region is illustrated in Fig. 1. The ideas of the shell model thus suggest that the wave functions of the lowest-lying energy levels of these nuclei should have the following characteristics: (1) an effectively closed and inert core of 82 neutrons; (2) an effectively closed and inert core of

50 protons; and (3) essentially complete vacancy of the proton orbits lying above the *gdhs* shell. Characteristics (2) and (3), of course, imply that those protons in excess of  $Z = 50$ , and only those, occupy the *gdhs* shell.

The present investigation was directed initially at testing these general hypotheses about the  $N = 82$  nuclei. Assuming their validity, it is apparent that a major theoretical simplification results from being able to treat the characteristics of the levels occurring at low excitation energies as arising solely from the interactions among from 3 to 13 protons within one major shell. For this reason it would appear that the  $N = 82$  isotones are one of the most appropriate regions in the Periodic Table in which to apply the techniques of the nuclear shell model to the problem of explaining experimental structure phenomena. Despite their potential theoretical importance, however, relatively little experimental work had been done on these nuclei until the last two years.<sup>5,6</sup> In particu-

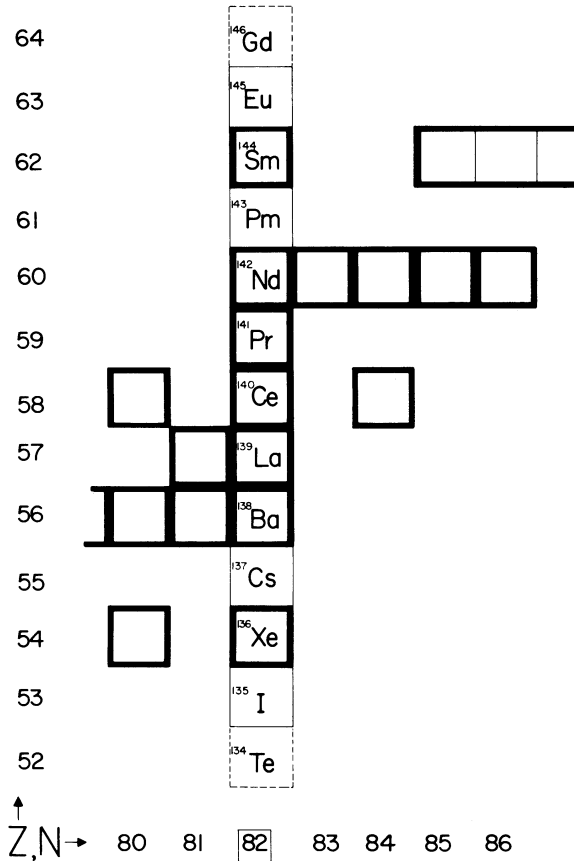


FIG. 1. Chart of the nuclides in the region of  $N = 82$ . Stable nuclei are heavily outlined, unstable nuclei whose properties have been studied are enclosed with thin solid lines, and nuclei as yet uninvestigated are outlined with dashed lines.

lar, proton-transfer data, essential in delineating the basic structural characteristics of the energy levels, were lacking. The measurements to be presented provide a significant improvement in

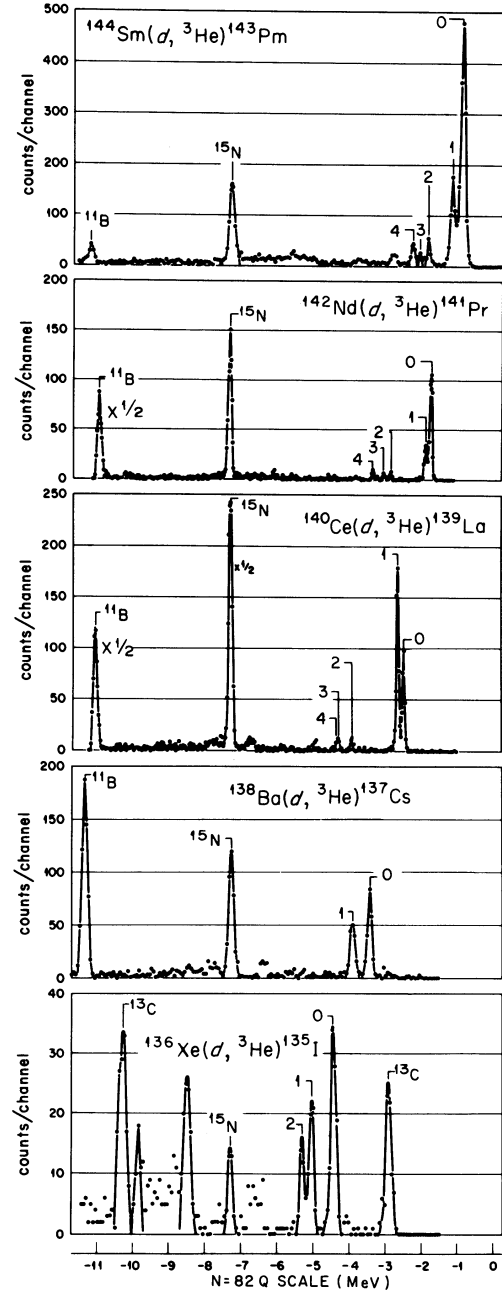


FIG. 2. Spectra of  ${}^3\text{He}$  particles detected at or near  $\theta_L = 20^\circ$  which result from deuteron bombardment of even-mass  $N = 82$  targets. The peaks of interest are denoted by numerals. The excitation energies of these states are listed, in their corresponding numerical order (0 = g.s., etc.), in the second column of Table III for each appropriate residual nucleus. Impurity peaks are specifically designated.

this situation. In an associated article the relationships between the present data and specific model calculations will be studied.<sup>7,8</sup>

## II. EXPERIMENTAL PROCEDURE

The measurements reported here were performed with the Oak Ridge Isochronous Cyclotron. The  $^3\text{He}$  spectra resulting from the deuteron bombardments were obtained with a standard solid-state particle detector  $\Delta E$ - $E$  telescope, combined with pulse-multiplier techniques. Typical energy resolution for the  $^3\text{He}$  particle groups was 90 keV, full width at half maximum (FWHM). The deuteron

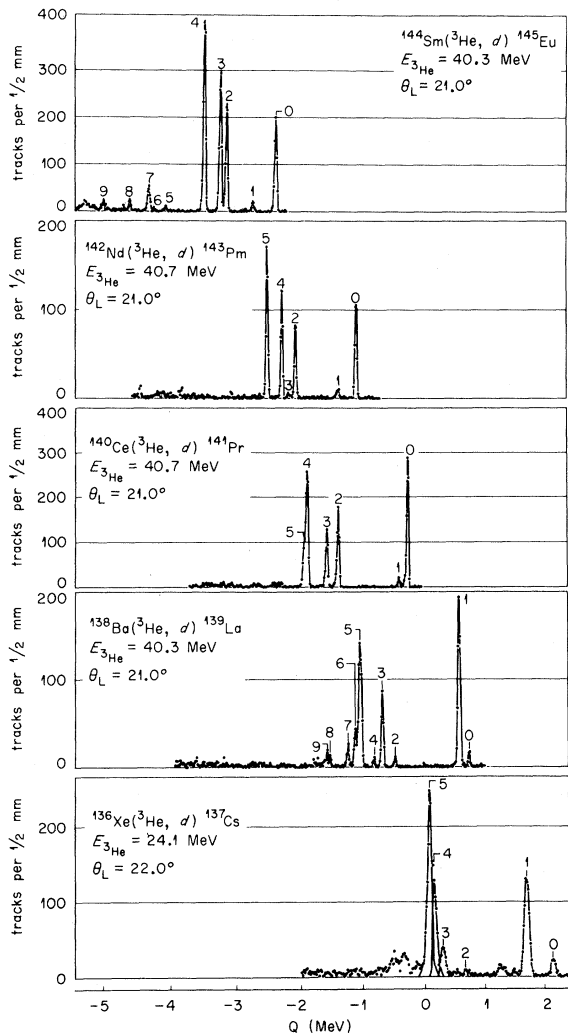


FIG. 3. Spectra of deuterons detected at or near  $\theta_L = 20^\circ$  which result from  $^3\text{He}$  bombardment of even-mass  $N=82$  targets. The peaks of interest are denoted by numerals. The excitation energies of these states are listed, in their corresponding numerical order (0 = g.s., etc.), in the second column of Table III for each appropriate residual nucleus.

bombarding energies were about 40 MeV. The spectra measured for each target near  $\theta_L = 20^\circ$  are shown in Fig. 2.

The deuteron spectra from the  $^3\text{He}$  bombardments were recorded in photographic emulsions placed in the focal plane of a broad-range magnetic spectrograph. Energy resolution for the particle groups in these spectra was about 35 keV FWHM. The spectra obtained for the various targets at about  $\theta_L = 20^\circ$  are shown in Fig. 3. The  $^3\text{He}$  bombardments were also at 40 MeV except for the case of the  $^{136}\text{Xe}$  target, where a 25-MeV beam was used. The use of the same energies for both the deuteron and  $^3\text{He}$  beams, and the relatively small range of the reaction  $Q$  values, produced a situation in which the incident channel for one set of reactions was very similar to the exit channels of the inverse set of reactions. Beam energies of 40 MeV were chosen in order to optimize the distinctiveness of the angular distributions of the various  $l_p$  transfers expected to be important in the "gdhs" shell.

The naturally occurring abundances of the  $N=82$  isotopes of the target elements are listed in the second column of Table I. The target materials used in the present experiments were enriched in the  $N=82$  isotopes to the values shown in the third column.<sup>9</sup> The  $Q$  values of the  $(d, ^3\text{He})$  and  $(^3\text{He}, d)$  reactions to the ground states of the respective  $(A-1)$  and  $(A+1)$  nuclei are listed in columns four and six of Table I, respectively. The  $^{136}\text{Xe}(d, ^3\text{He})$ - $^{135}\text{I}$  and the  $^{142}\text{Nd}(^3\text{He}, d)^{143}\text{Pm}$   $Q$  values were obtained from the present series of measurements. Other masses were known to within the accuracies attainable in the present experiments and the listed values are taken from the tables of Mattauch, Thiele, and Wapstra.<sup>10</sup> The  $Q$  values for the  $(d, ^3\text{He})$  and  $(^3\text{He}, d)$  reactions on  $^{16}\text{O}$  and  $^{12}\text{C}$ , the dominant contaminants in all of the targets except  $^{136}\text{Xe}$ , are also given in Table I. It can be seen that these contaminants do not pose a serious problem for most of the low-energy spectra of the residual  $N=82$  nuclei. The specific bombarding energies used in the various experiments are listed in columns 5 and 7 of Table I.

The targets of  $^{138}\text{Ba}$ ,  $^{140}\text{Ce}$ , and  $^{142}\text{Nd}$  were each prepared by reducing the isotopically enriched carbonate to the oxide in a tantalum-tube furnace under vacuum. The oxides were then evaporated by electron bombardment from a carbon boat onto very thin carbon backings. Target thicknesses exclusive of the backings ranged between 50 and 300  $\mu\text{g}/\text{cm}^2$ . The  $^{144}\text{Sm}$  target was a self-supporting rolled foil of 500  $\mu\text{g}/\text{cm}^2$  areal density. The Xe gas was contained in a 3-in.-diam cell modeled after one designed by Jones and Mancusi.<sup>11</sup> Havar entrance and exit windows were 0.0001 in. thick

TABLE I. Target and reaction information.

Element	Natural (%)	Enriched (%)	$Q(d, {}^3\text{He})$ (MeV)	$E_d$ (MeV)	$Q({}^3\text{He}, d)$ (MeV)	$E_{{}^3\text{He}}$ (MeV)
${}^{136}\text{Xe}$	8.9	90 <sup>a</sup> –95 <sup>b</sup>	$-4.438 \pm 0.040$	40.3	$2.216 \pm 0.070$	24.1
${}^{138}\text{Ba}$	71.7	99.8	$-3.463 \pm 0.070$	40.3	$0.734 \pm 0.032$	40.3
${}^{140}\text{Ce}$	88.5	99.7	$-2.493 \pm 0.048$	40.3	$-0.258 \pm 0.010$	40.7
${}^{142}\text{Nd}$	27.1	97.7	$-1.732 \pm 0.010$	40.3	$-1.099 \pm 0.025$	40.7
${}^{144}\text{Sm}$	3.1	94.5	$-0.661 \pm 0.030$ <sup>c</sup>	40.3	$-2.203 \pm 0.050$	40.3
${}^{16}\text{O}$	...	...	$-6.632 \pm 0.001$	...	$-4.893 \pm 0.001$	...
${}^{12}\text{C}$	...	...	$-10.463 \pm 0.001$	...	$-3.550 \pm 0.001$	...

<sup>a</sup>For ( ${}^3\text{He}, d$ ).<sup>b</sup>For ( $d, {}^3\text{He}$ ).<sup>c</sup>Derived from  ${}^{142}\text{Nd}({}^3\text{He}, d){}^{143}\text{Pm}$  measurement.

and pressures of about  $\frac{1}{10}$  atmosphere were employed. These pressures, coupled with the slit system used, were equivalent to a target thickness of about  $100 \mu\text{g}/\text{cm}^2$ . The several types of targets and their different thicknesses produced spectra of varying quality.

Differential cross sections were usually measured to about  $40^\circ$ . The rapid decrease of reaction intensities as the angle to the beam increased made measurements at larger angles prohibitively time consuming. And, in any case, the data at large angles have essentially no bearing on the spectroscopic information of interest in the present study. The smallest angle at which data were taken was  $5^\circ$  for the ( ${}^3\text{He}, d$ ) experiments and  $11^\circ$  for the ( $d, {}^3\text{He}$ ) experiments. The high counting rates of elastically scattered deuterons in the solid-state detectors made taking ( $d, {}^3\text{He}$ ) data at smaller angles impractical even though such information would have been useful.

In the present work it was not feasible to make an absolute determination of the cross sections for a particular target to an accuracy of better than 25%. The cross sections for one target relative to another had the same sort of uncertainty. The procedure by which the experimental cross sections were related to the DWBA calculated cross sections is discussed in the next section.

### III. DISTORTED-WAVE ANALYSIS

#### A. Optical-Model Potentials and Predicted Angular Distributions

From the discussion in the Introduction, it is to be expected that the proton transfers occurring via the ( ${}^3\text{He}, d$ ) and ( $d, {}^3\text{He}$ ) reactions on  $N=82$  targets will involve  $l_p$  values of 4, 2, 5, and 0. The differential cross sections for these transfers were calculated in the local, zero-range (LZR) approximation of the DWBA with the code JULIE.<sup>12</sup> The choice of bombarding energies made a rigid consistency in the DWBA calculations possible. The same deuteron optical-model potential and the same  ${}^3\text{He}$  optical-model potential were used in all of the calculations. The deuteron parameters are those deduced by Newman *et al.*<sup>13</sup> from the analysis of 34-MeV deuteron elastic scattering data. The  ${}^3\text{He}$  parameters are based on those obtained by Gibson *et al.*<sup>14</sup> from the analysis of  ${}^3\text{He}$  elastic scattering on several medium-mass targets at energies in the 30–60-MeV range. All of the parameters which enter into the DWBA calculations are listed in Table II. The shapes and intrinsic magnitudes of the angular distributions calculated in the DWBA for the four values of  $l_p$  are shown in Fig. 4. The curves result from calculations which assume the ( ${}^3\text{He}, d$ ) reaction on

TABLE II. Optical-model potentials.

	$V$ (MeV)	$r_0$ (F)	$r_{0c}$ (F)	$a$ (F)	$W$ (MeV)	$r_0'$ (F)	$a'$ (F)	$W_D$ (MeV)
Deuteron	99.0	1.12	1.30	0.820	...	1.24	0.86	15.75
${}^3\text{He}$	175.0	1.14	1.40	0.723	17.5	1.60	0.86	...
Bound state (centroid)	(Separation energy prescription)	1.24	1.25	0.65	...	...	...	...
Bound state (spin-orbit)	( $\lambda=20$ )	1.14	...	0.65	...	...	...	...

$^{140}\text{Ce}$  with a  $Q$  value of 0.0 MeV. It can be seen that the curves for the various  $l_p$  transfers are quite distinctive from one another, and that each is uniquely identified by the portion of the curve

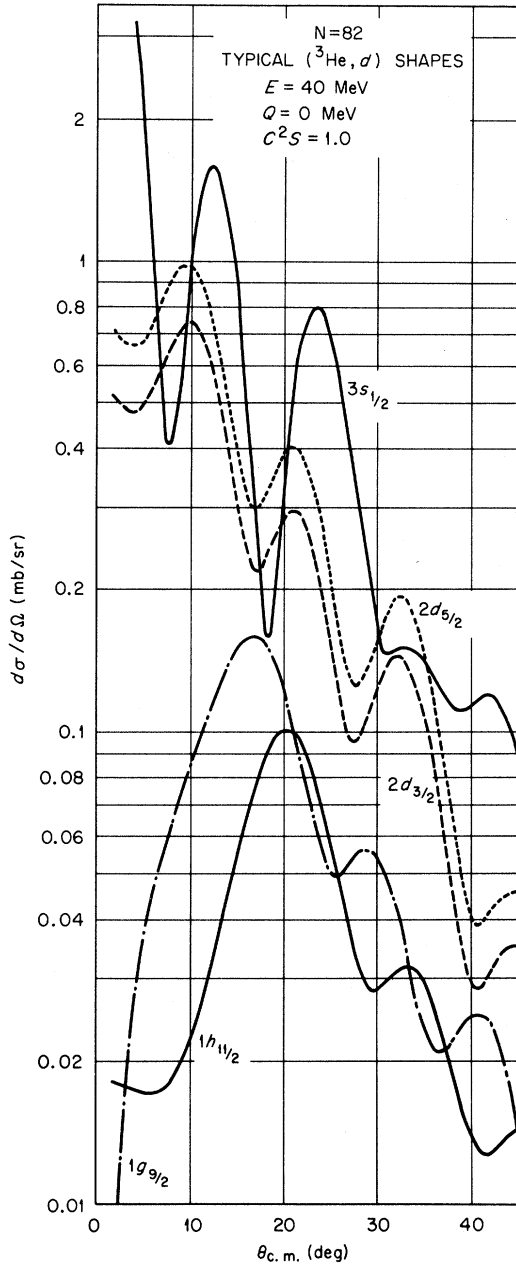


FIG. 4. Shapes of DWBA predictions for transitions involving the orbits which are filled between  $Z=51$  and  $82$ . The calculations assume  $(^3\text{He}, d)$  stripping at  $40$  MeV on  $^{140}\text{Ce}$  with a  $Q$  value of  $0.00$  MeV and the quantum numbers associated with the various curves. The absolute cross sections are plotted so as to reflect the relative intrinsic cross sections of the various  $l$  transfers. The values result from the standard version of the calculations.

between  $10$  and  $35^\circ$ . It follows that for the process of assigning  $l_p$  values to experimental angular distributions by matching them to the DWBA curves, experimental data in this angular range are sufficient. It can also be seen that to achieve the desired goal of matching theoretical to experimental cross sections at the angles of maximum cross section, data from  $5$  to  $10^\circ$  are desirable for the cases of  $l_p = 2$  and, in particular,  $l_p = 0$  transitions.

#### B. Predicted Cross Sections from the DWBA and Parameters of the "Bound-State Well"

The differential cross sections obtained from the DWBA calculations are interpreted as corresponding to the stripping (pickup) of a particle into (out of) a single-particle orbit ( $nlj$ ) under the condition that the other nucleons in the target nucleus (which are inequivalent to the transferred particle) from an inert core which is identical in the initial and final states. The bound-state wave function for the transferred nucleon is obtained by assuming the orbit to be an eigenfunction of a Woods-Saxon potential well with an energy eigenvalue equal to the experimentally observed separation energy for the nucleon in question. The form of the well is

$$V(r) = V_0(r) + V_{\text{so}}(r) + V_{\text{Coul.}}(r), \quad (1)$$

where

$$V_0(r) = -V_0 f(r); \quad (2a)$$

$$V_{\text{so}}(r) = -\lambda V_0 (\hbar/2M_p c)^2 \vec{I} \cdot \vec{\sigma} r^{-1} df'(r)/dr; \quad (2b)$$

$$V_{\text{Coul.}}(r) = Ze^2(3 - r^2/R_0^2)/2R_0, \quad r < r_c A^{1/3}; \quad (2c)$$

$$= Ze^2/r, \quad r > r_c A^{1/3};$$

and

$$f(r) = \left[ 1 + \exp\left(\frac{r - r_0 A^{1/3}}{a_0}\right) \right]^{-1} \quad (3a)$$

$$f'(r) = \left[ 1 + \exp\left(\frac{r - r_{\text{so}} A^{1/3}}{a_{\text{so}}}\right) \right]^{-1} \quad (3b)$$

One aspect of the calculations which strongly affects the magnitude of the predicted cross sections, but only minimally affects the relative cross sections for different ( $nlj$ ) transfers, is the radius parameter,  $r_0$ , of the central part of the bound-state well. Changes of  $5\%$  in the bound-state radius for  $(d-^3\text{He})$  transfer reactions can produce  $30\%$  changes in the predicted cross sections.<sup>15</sup> Increased radii correspond to larger expectation values for the transferred particle at the absorption surface and hence to larger cross sections. The value of  $r_0$  which, together with the "Bassel normalization"<sup>16</sup> of the  $(d-^3\text{He})$  overlap, seems to give consistency between LZR DWBA analyses of

data and general sum-rule expectations is about 1.24 F.<sup>17</sup> Our results are, within the experimental uncertainties, consistent with the  $r_0 = 1.24$  F-“Bassel normalization” combination.

There is another, less well known, aspect of the DWBA calculations which is particularly important for the strongly surface-dominated ( $d$ - $^3\text{He}$ ) processes. This concerns the use of the spin-orbit term in the bound-state well of Eq. (1). For the same value of the transferred orbital angular momentum  $l$ , the spin-orbit term causes those transitions with  $j = l + \frac{1}{2}$  to have larger predicted cross sections than those with  $j = l - \frac{1}{2}$ . This results from the fact that the spin-orbit term is acting at the edge of the nucleus, pushing the wave function of the bound particle inwards for the  $j = l - \frac{1}{2}$  case and pulling it outward for the  $j = l + \frac{1}{2}$  case. In the traditional use of the DWBA, the geometrical parameters of the spin-orbit and central wells [Eqs. (2a) and (2b)] are constrained to the same values, i.e.,  $r_{so} = r_0$  and  $a_{so} = a_0$ .

A study of the single-particle states in  $^{209}\text{Bi}$  via the  $^{208}\text{Pb}(^3\text{He}, d)^{209}\text{Bi}$  reaction<sup>18</sup> has shown that the conventional prescription for introducing spin-orbit effects produces too large a difference between the cross sections of  $j = l + \frac{1}{2}$  and  $j = l - \frac{1}{2}$  transitions. The effect is, of course, strongly dependent upon  $l$  and hence showed up clearly in the  $l = 3, 5,$  and  $6$  transitions to  $^{209}\text{Bi}$ . Subsequent investigations<sup>19</sup> have shown that making the spin-orbit radius about 10% smaller than that of the central well radius ameliorates this problem. This prescription is suggested by and consistent with the findings of various recent nucleon-nucleus scattering studies.<sup>20</sup>

As may be expected, the  $l = 4, j = \frac{7}{2}$  cross sections of ( $^3\text{He}, d$ ) transitions in the  $N = 82$  region are quite sensitive to this effect. The cross section from the calculation with a reduced spin-orbit radius is a factor of  $\sim 1.20$  larger than that from the conventional calculation, all other aspects being held constant. The changes in the cross sections resulting from this modification in the DWBA calculations for the other transfers are as follows:  $2d_{5/2} \sim 0.93$ ,  $1h_{11/2} \sim 0.82$ , and  $2d_{3/2} \sim 1.11$ . Thus, the modified DWBA analysis produces significantly different results from the standard analysis. We will present results from both procedures.

### C. Spectroscopic Factors

The effects of the nuclear structure of the initial and final energy levels involved in a particular direct-reaction transition manifest themselves as a ratio of the experimentally measured differential cross sections to the pertinent intrinsic cross sections calculated in the DWBA. The experimentally

observed transition is identified as to  $l_p$  by finding a match between its angular distribution and the curves calculated for various values of  $l_p$ . The complete ( $nlj$ ) specification for the transition (if otherwise unknown) is then arrived at, if possible, by a combination of assumptions and deductions based on general shell-model ideas. An index of the structural details affecting the strength of the particular transition, called the spectroscopic factor  $S(nlj)$ , is then extracted on the basis of the following equations<sup>12</sup> for, respectively, ( $^3\text{He}, d$ ) and ( $d, ^3\text{He}$ ) reactions:

$$\frac{d\sigma(\theta)}{d\Omega}(nlj)_{\text{exp}} = \frac{2J_f + 1}{2J_i + 1} S(nlj) N(^3\text{He}, d) \frac{d\sigma(\theta)}{d\Omega}(nlj)_{\text{DW}} \quad (4)$$

and

$$\frac{d\sigma(\theta)}{d\Omega}(nlj)_{\text{exp}} = S(nlj) N(d, ^3\text{He}) \frac{d\sigma(\theta)}{d\Omega}(nlj)_{\text{DW}}. \quad (5)$$

The factors “ $N$ ” account for the overlap and statistics of the ( $d$ - $^3\text{He}$ ) aspect of the reaction cross sections,<sup>16</sup> and  $J_i$  and  $J_f$  refer to the spins of the initial and final nuclear states.

The stripping spectroscopic factor corresponds theoretically to the expectation value between the initial and final wave functions of a particle-creation operator of the correct ( $nlj$ ) quantum numbers. The pickup spectroscopic factor corresponds to the analogous particle-destruction operator. As such, the spectroscopic factor yields a measure of the overlap of the final state with the wave function formed by coupling a single particle or hole to the initial state. Also, the sum of all  $S$ -factor strength for a particular ( $nlj$ ) provides a measure of the occupation (vacancy) probability of that orbit in the target ground state.<sup>21</sup>

The occupation probabilities for the various active orbits in the target states thus can be obtained either from the ( $d, ^3\text{He}$ ) experiments – measuring occupancies – or from the ( $^3\text{He}, d$ ) experiments – measuring the complementary vacancies. A consistent set of answers from the two approaches is a fundamental test of the internal consistency of the DWBA analysis. In this regard we will find that the DWBA calculations modified to use reduced spin-orbit radii are significantly better than the standard version. Inconsistency between stripping and pickup results manifests itself as follows. The usual analysis yields spectroscopic factors that are too small for  $j = l - \frac{1}{2}$  transitions (spectroscopic factors being inversely proportional to DWBA cross sections). Thus, for the  $1g_{7/2}$  orbit, the pick-up results would yield too small an occupation probability while the stripping results would indicate too small a vacancy, which corresponds to too *large* an occupation probability. The effects

propagate through the other orbits. Since we will be dealing with relative spectroscopic factors, this problem shows up, for example, as inconsistent ratios for the  $1g_{7/2}-2d_{5/2}$  occupation probabilities as determined via the complementary pick-up and stripping reactions on a given target. By reducing the effect of the spin-orbit potential on cross sections, the modified DWBA analysis produces results from stripping and pick-up reactions on a given target which are more consistent with each other.

Even under the best possible conditions, however, there are probably still uncertainties in relative spectroscopic factors of 15%. This sort of uncertainty can, in some cases, lead to much larger percentage errors in the extraction of occupation probabilities. For example, an important question in the present study concerns the occupation of the  $1h_{11/2}$  orbit in the target ground states. The  $(d, {}^3\text{He})$  spectroscopic factor for the  $\frac{1}{2}^-$  state in the various residual nuclei gives a direct value for this quantity. However, since the occupation probability is small and in addition the intrinsic cross section for  $l_p = 5$  is weak (see Fig. 4), the observed cross sections are small, and accurate values for the pick-up  $S$  factors are difficult to obtain for purely experimental reasons. Conversely, stripping into the  $1h_{11/2}$  vacancy yields much larger cross sections and the  $S$  factors can be extracted with good experimental accuracy. For  $(nlj) = (1, 5, \frac{1}{2}^-)$ ,  $S = 0.9$ , the occupation probability,  $\langle 1h_{11/2} \rangle$ , is 1.2. Considering the 15% uncertainty inherent in  $S$ , however, we see that the value of  $\langle 1h_{11/2} \rangle$  could, in this example, legitimately range between 0 and 2.8. The ubiquity of this type of problem carries the implication that measurements of "small" effects of the sort illustrated will have inherent uncertainties of the order of a factor of 2.

#### D. Normalization of Spectroscopic Factors

As was mentioned, the absolute cross sections for a given reaction and target contained large uncertainties. It follows that individual absolute spectroscopic factors could not be extracted with good accuracy. We have chosen to normalize the  $S(nlj)$  so as to illuminate the *internal* consistency of the DWBA-extracted results. One of the most striking features of the  $({}^3\text{He}, d)$  spectra of Fig. 3 is the concentration of transition intensity into the low-lying states. It appears to be a secure assertion that the preponderance of the spectroscopic strength to the empty "*gdhs*" orbits is contained in the analyzed angular distributions. We assume here that all of the observed stripping transitions proceed to orbits of the "*gdhs*" shell and that all of the target protons in excess of 50 also occupy orbits of this shell. Under these conditions, a gen-

eral limitation on the sum of the stripping strength to "*gdhs*" states exists and has the form

$$\sum_{\substack{n,l,j \in \text{"gdhs"} \\ i \in \text{obs. states}}} (2j+1)S_i(nlj) \leq (32 - [Z - 50]), \quad (6)$$

where  $Z$  is the proton number of the  $N=82$  target nucleus. This sum rule expresses the fact that protons can be created and coupled to an  $N=82$  nuclear ground state only to the extent that its wave function has proton holes remaining in the "*gdhs*" shell. To the extent that the *observed* stripping strength corresponds to the total existing, the inequality (6) approaches equality.

For our purposes here we *assume* that all of the stripping transitions have been observed, and correspondingly choose a normalization for the  $({}^3\text{He}, d)$  spectroscopic factors on a given target such that the equality in formula (6) holds. By this procedure, we impose a normalization on the experimental  $({}^3\text{He}, d)$  results for each of the  $N=82$  targets, and the tabulated spectroscopic factors are based on these normalizations. Now if the DWBA analysis for a set of stripping transitions from a given target was completely consistent, no spectroscopic sum for a particular  $(nlj)$  would exceed unity. The cases in which this rule is violated thus yield an estimate of the minimum uncertainty of the DWBA analysis. There are a multiplicity of other criteria that could be used to choose a normalization, e.g., imposing the conditions just stated, that no orbit have a  $\sum_i (n, l, j)$  greater than unity. We chose the one previously described because we felt it averaged over the various calculations and data best. However, in some cases the results lead to "supervacancy" for orbits that the complementary pickup reaction shows to be populated to some extent.

The  $(d, {}^3\text{He})$  spectroscopic factors were normalized to be consistent with the  $({}^3\text{He}, d)$  results for the same target nuclei. The sum of the pickup strength to the lowest  $\frac{7}{2}^+$  and  $\frac{5}{2}^+$  states was adjusted so as to yield a combined  $(1g_{7/2} - 2d_{5/2})$  occupation probability consistent with that deduced from the stripping measurements. Thus, from stripping,

$$\langle 1g_{7/2} + 2d_{5/2} \rangle = \sum_j (1 - \sum_i S_i(j))(2j+1), \quad (7)$$

and from pickup,

$$\langle 1g_{7/2} + 2d_{5/2} \rangle = \sum_{i,j} S_i(j), \quad (8)$$

where in each case " $j$ " can equal  $\frac{7}{2}$  and  $\frac{5}{2}$  and " $i$ " runs over all observed states of a particular " $j$ ". Hence, the pick-up spectroscopic factors were normalized to the stripping results by requiring equality between Eqs. (7) and (8). We emphasize

that the significant aspects of the spectroscopic factors to be presented lie in their values *relative* to one another.

#### IV. RESULTS AND DISCUSSIONS

##### A. General Remarks

The spectra of observed particles from the ( $d, {}^3\text{He}$ ) and ( ${}^3\text{He}, d$ ) reactions on the even  $N=82$  targets have been presented in Figs. 2 and 3, respectively. Each of the ( $d, {}^3\text{He}$ ) spectra in Fig. 2 shows evidence for only two transitions of major strength in the first 3 MeV of excitation. On the other hand, each of the ( ${}^3\text{He}, d$ ) spectra of Fig. 3 shows at least five transitions with significant intensity in the same region. As will be seen in the detailed exposition which follows, one of the two strong groups observed in each of the pick-up reactions has an  $l_p=2$  shape and the other an  $l_p=4$  shape. The ideas developed in the preceding sections lead to the following conclusions. The presence of only two kinds of transitions in the pick-up spectra (a first approximation) implies that only two active orbits in the target state have appreciable occupation probability. The ordering of single-particle states in the "shell-model" potential well then requires that the  $l_p=4$  transitions be associated with the  $1g_{7/2}$  orbit, since  $1g_{9/2}$  protons should be tightly bound in the  $Z=50$  core. Both  $2d_{5/2}$  and  $2d_{3/2}$  orbits occur in the  $gdhs$  shell, but if only one orbit is occupied, it should on all counts be that with  $j=l+\frac{1}{2}$ . Hence, the general conclusion to be drawn from the pick-up studies is that in the target ground states the protons outside  $Z=50$  occupy  $1g_{7/2}$  and  $2d_{5/2}$  orbits. This is in fact consistent with the more detailed predictions of the shell-model ordering schemes and with other experimental studies of the ground- and first excited-state spins of some of the odd-mass nuclei.<sup>5,6</sup>

The strong states observed in the stripping spectra have angular distributions characterized by  $l_p=0, 2, 4,$  and  $5$ . The lowest  $l_p=2$  transition corresponds to the  $l_p=2$  state seen in the pickup transition to the same nucleus. Hence, it follows that it must also correspond to transfer of a  $2d_{5/2}$  proton. Similarly, the  $l_p=4$  stripping transition populates the same states that is formed by  $l_p=4$  pick-up. In addition to these two states, each stripping spectrum has a single transition characterized by  $l_p=5$  and one each (or a set of fragments thereof) characterized by  $l_p=0$  and  $l_p=2$ . It is consistent with our previous discussion to assume that these higher states (or centroids in the cases of fragmentation) correspond to the remaining three single-particle orbits in the  $gdhs$  shell, namely  $1h_{11/2}$ ,  $2s_{1/2}$ , and  $2d_{3/2}$ .

Our simple expectations about the structure of

the levels of  $N=82$  nuclei at low excitation energies are confirmed by this initial inspection of the experimental results. Levels in the odd-mass nuclei whose wave functions might involve the proton orbits above  $Z=82$  would be characterized by stripping transitions of  $l_p=5, 3,$  and  $1$  (corresponding to the  $1h_{9/2}, 2f,$  and  $3p$  orbits). No transitions with  $l_p=1$  or  $3$  are observed. The single  $l_p=5$  transition observed for any one nucleus must logically be associated with the  $1h_{11/2}$  member of the  $gdhs$  shell rather than the  $1h_{9/2}$  member of the shell above  $Z=82$ , since the pickup results indicate neither "h" orbit is significantly occupied. Levels arising from configurations involving the excitation of protons out of the orbits below  $Z=50$  would be populated by pick-up transitions of  $l_p=4, 3,$  or  $1$ , corresponding to the  $1g_{9/2}, 1f,$  and  $2p$  orbits. Again, no  $l=3$  or  $1$  transitions are seen, and the single  $l_p=4$  transition must be associated with the  $1g_{7/2}$  orbit of the  $gdhs$  shell, since stripping indicates only one "g" orbit is unfilled, and this one must be the higher-lying,  $j=l-\frac{1}{2}$  member. Hence, the final states populated by ( ${}^3\text{He}, d$ ) or ( $d, {}^3\text{He}$ ) are all explicable in terms of  $gdhs$  configurations. The same general evidence can be used to conclude that the target ground states are also constructed from within the  $gdhs$  shell, with the  $Z\leq 50$  and  $Z\geq 82$  shells effectively completely full and completely empty, respectively.

The angular distributions of the ( $d, {}^3\text{He}$ ) reactions on the various even-mass  $N=82$  targets are shown in Figs. 6, 8, 10, 12, and 14, while the ( ${}^3\text{He}, d$ ) angular distributions for the same target nuclei are shown in Figs. 7, 9, 11, 13, and 15. The curves are the DWBA predictions for the individual transitions, and the fits of the calculated shapes to the data points are the basis of the assignments of  $l_p$ .

Table III lists the excitation energies of the various levels of the odd-mass  $N=82$  nuclei which are observed in the present experiments. Because of the better energy resolution and statistical accuracy of the ( ${}^3\text{He}, d$ ) data, the excitation energies are taken from the ( ${}^3\text{He}, d$ ) data except for  ${}^{135}\text{I}$ , where of course none were available. Also listed in this table are the assigned values of  $l_p$ , the assumed values of  $J$ , and the spectroscopic factors  $S(nlj)$  extracted from both the ( ${}^3\text{He}, d$ ) and ( $d, {}^3\text{He}$ ) angular distributions. Results from both the standard and the modified DWBA analyses are included.

##### B. Details of Results

###### 1. ${}^{136}\text{Xe}(d, {}^3\text{He}){}^{135}\text{I}$

Prior to the present experiment, the only definite information available about  ${}^{135}\text{I}$ , the lightest

TABLE III. Excitation energies,  $l_p$  values, and spectroscopic factors for levels of odd-mass  $N = 82$  nuclei excited by proton stripping and pick-up reactions. Uncertainties in measured excitation energies are 8 keV per MeV of excitation.

Residual nucleus	Measured excitation energy (MeV)	$l_p$	$J^\pi$ Assumed	$S(n, l, j)$ ( $^3\text{He}, d$ )		$S(n, l, j)$ ( $d, ^3\text{He}$ )	
				Mod.	Stand.	Mod.	Stand.
$^{135}\text{I}$	0.00	4	$\frac{7}{2}^+$			2.74	1.82
	$0.590 \pm 0.030$	2	$\frac{5}{2}^+$			0.34	0.17
	$0.860 \pm 0.040$	2	$\frac{5}{2}^+$			0.12	0.06
$^{137}\text{Cs}$	0.00	4	$\frac{7}{2}^+$	0.60	0.75	3.91	3.57
	0.455	2	$\frac{5}{2}^+$	1.02	0.99	1.01	0.71
	1.49	0	$\frac{1}{2}^+$	0.07	0.07		
	1.87	5	$\frac{11}{2}^-$	1.01	0.87		
	2.07	2	$\frac{3}{2}^+$	0.79	0.92		
	2.15	0	$\frac{1}{2}^+$	0.86	0.89		
$^{139}\text{La}$	0.00	4	$\frac{7}{2}^+$	0.43	0.54	6.21	6.07
	0.166	2	$\frac{5}{2}^+$	0.94	0.90	1.71	1.29
	1.21	0	$\frac{1}{2}^+$	0.09	0.10		
	1.42	5	$\frac{11}{2}^-$	0.84	0.71	0.7	0.6
	1.56	2	$\frac{3}{2}^+$	0.06	0.07		
	1.78	0	$\frac{1}{2}^+$	0.65	0.67		
	1.78	2	$\frac{3}{2}^+$	0.73	0.83		
	1.85	2	$\frac{3}{2}^+$	0.26	0.30		
	1.96	2	$\frac{3}{2}^+$	0.16	0.19		
	2.24	2	$\frac{3}{2}^+$	0.08	0.10		
	2.31	0	$\frac{1}{2}^+$	0.13	0.13		
$^{141}\text{Pr}$	0.00	2	$\frac{5}{2}^+$	0.64	0.64	2.70	2.12
	0.145	4	$\frac{7}{2}^+$	0.28	0.35	6.06	6.20
	1.11	5	$\frac{11}{2}^-$	0.96	0.84	1.03	0.86
	1.30	0	$\frac{1}{2}^+$	0.61	0.65	0.09	0.09
	1.60	2	$\frac{3}{2}^+$	1.04	1.23		
	1.65	0	$\frac{1}{2}^+$	0.51	0.54		
$^{143}\text{Pm}$	0.00	2	$\frac{5}{2}^+$	0.54	0.52	3.80	3.20
	0.270	4	$\frac{7}{2}^+$	0.25	0.32	6.85	7.50
	0.96	5	$\frac{11}{2}^-$	0.82	0.71	1.65	1.40
	1.06	2	$\frac{3}{2}^+$	0.05	0.06		
	1.17	0	$\frac{1}{2}^+$	1.08	1.12	0.23	0.23
	1.40	2	$\frac{3}{2}^+$	1.13	1.31	0.48	0.53
$^{145}\text{Eu}$	0.00	2	$\frac{5}{2}^+$	0.33	0.33		
	0.329	4	$\frac{7}{2}^+$	0.17	0.22		
	0.716	5	$\frac{11}{2}^-$	0.83	0.72		
	0.808	0	$\frac{1}{2}^+$	1.00	1.05		

TABLE III (Continued)

Residual nucleus	Measured excitation energy (MeV)	$l_p$	$J^\pi$ Assumed	$S(n, l, j)$ ( $^3\text{He}, d$ )		$S(n, l, j)$ ( $d, ^3\text{He}$ )	
				Mod.	Stand.	Mod.	Stand.
	1.04	2	$\frac{3}{2}^+$	1.03	1.21		
	1.76	2	$\frac{3}{2}^+$	0.02	0.05		
	1.84	2	$\frac{3}{2}^+$	0.10	0.12		

$N=82$  nucleus that can be studied with current techniques, was that its ground state had  $J^\pi = \frac{7}{2}^+$ . The uncertainty in its mass was listed<sup>9</sup> as 1 MeV.

The ( $d, ^3\text{He}$ ) reaction cross sections on  $^{136}\text{Xe}$  are quite small. This results from the fact that there are only four active protons in the ground state and these predominantly occupy the  $1g_{7/2}$  orbit, for which the intrinsic transfer cross section is quite weak. Compounding the experimental problems for this reaction was the fact that energy resolution in the spectra was appreciably poorer than in the other ( $d, ^3\text{He}$ ) experiments because of straggling in the gas cell windows and in the gas. Data from the  $^{136}\text{Xe}(d, ^3\text{He})^{135}\text{I}$  reaction were accumulated over a period of three days, during which the target gas was left undisturbed. At least two spectra were accumulated at each angle at separate times, so as to provide information on possible contaminant accumulation. No change in the target gas could be detected.

A spectrum of the  $^3\text{He}$  events from the  $^{136}\text{Xe}$  target is shown in Fig. 5. The three labeled peaks are interpreted as corresponding to the ground, first excited and second excited states of  $^{135}\text{I}$ . The

angular distributions of the transitions to these levels are shown in Fig. 6. The ground-state distribution agrees with an  $l_p = 4$  DWBA curve and the excited-state distributions are each in agreement with  $l_p = 2$  curves. The energies of the excited states are listed in Table III. In order to establish the  $Q$  value for the ground-state transition without first-order dependence on beam energy and the thicknesses of the target gas, cell window, etc., the  $^{136}\text{Xe}$  target was deliberately contaminated with a charge of air at the end of the experiment. Spectra at several angles were accumulated with the particle groups from the  $^{14}\text{N}(d, ^3\text{He})^{13}\text{C}$  and  $^{16}\text{O}(d, ^3\text{He})^{15}\text{N}$  reactions superimposed upon the  $^{135}\text{I}$  spectrum. One of these spectra is shown in Fig. 2. Since all the particles had passed through the identical environment, the  $Q$  value for  $^{136}\text{Xe}(d, ^3\text{He})^{135}\text{I}$  was immediately established by reference to the known  $Q$  values of the reactions on  $^{16}\text{O}$  and  $^{14}\text{N}$  and the appropriate kinematic corrections. The new measured value is listed in Table I. As will be discussed later, both of the  $l_p = 2$  transitions were assumed to correspond to pickup of  $2d_{5/2}$  protons, and the spectroscopic factors listed in Table III

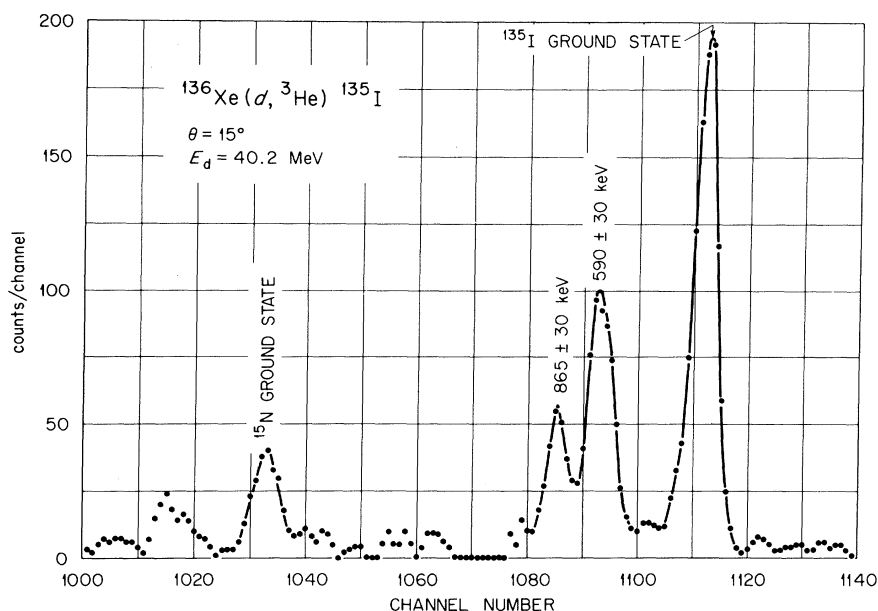


FIG. 5. Spectrum of  $^3\text{He}$  particles emitted in the  $^{136}\text{Xe}(d, ^3\text{He})^{135}\text{I}$  reaction.

were extracted on this basis.

### 2. $^{136}\text{Xe}(^3\text{He}, d)^{137}\text{Cs}$

The data for the  $(^3\text{He}, d)$  reaction on  $^{136}\text{Xe}$  were taken at a bombarding energy of 25 MeV rather than 40 MeV because of technical difficulty with the cyclotron beam during that particular experimental period. This had two effects, the first being that energy straggling in the windows and tar-

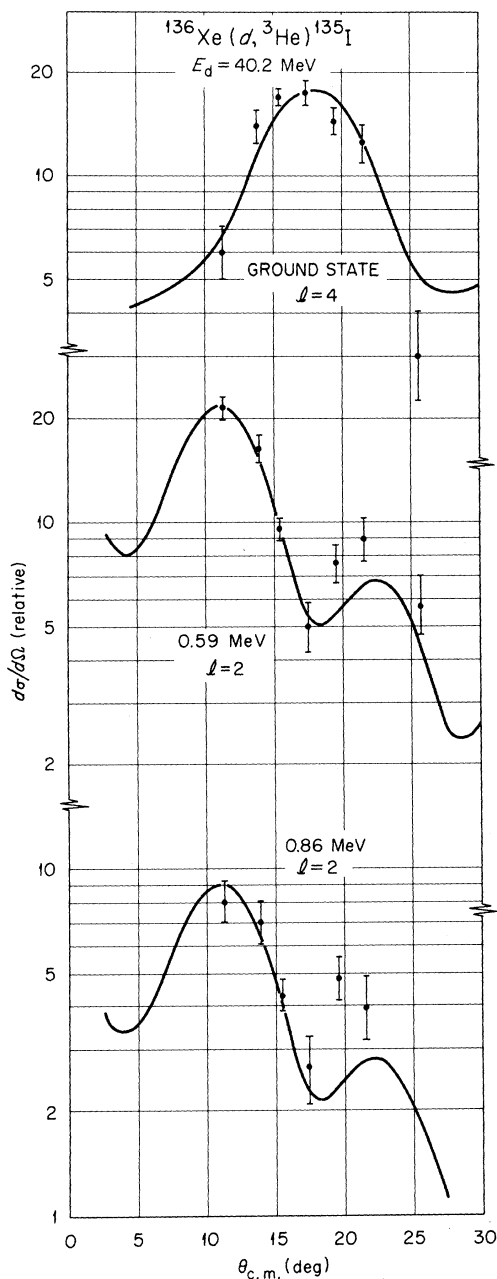


FIG. 6. Angular distributions of the first three transitions observed in the  $^{136}\text{Xe}(d, ^3\text{He})^{137}\text{I}$  reactions. The curves are DWBA predictions.

get gas was relatively more severe than would have been the case at 40 MeV and the second being that the extraction of spectroscopic factors with the 40-MeV families of optical-model parameters was subject to additional uncertainties compared to the other sets of experimental data.

A sample spectrum of the reaction is shown at the bottom of Fig. 3. The angular distributions of the six groups to which energies are assigned in Fig. 3 are shown in Fig. 7, together with the DWBA calculations. The ground-state transition is  $l_p = 4$  and the first excited state is  $l_p = 2$ . The spectroscopic factors are consistent with these two levels being formed by coupling  $1g_{7/2}$  and  $2d_{5/2}$  protons, respectively, to the  $^{136}\text{Xe}$  ground state. We will in the following discussion refer to this sort of level as a " $(nlj)$ -single-particle (hole) state." A weakly excited level at 1.49 MeV has an  $l_p = 0$  angular distribution, as does a much stronger transition to a level at 2.15 MeV. Levels at 1.87 and 2.07 MeV are populated by  $l_p = 5$  and 2 transitions, respectively. The spectroscopic factors suggest the assignment of  $J = \frac{3}{2}$ , and a  $2d_{3/2}$ -single-particle nature, for the 2.07-MeV state and  $1h_{11/2}$  and  $3s_{1/2}$  single-particle characters for the 1.87- and 2.15-MeV levels, respectively. It is possible that states in the vicinity of 800 keV are populated also, but the reaction events in this region which are observable in Fig. 3 cannot definitely be attributed to any one unique parent.

In a recent study<sup>22</sup> of the  $\gamma$  rays which follow the  $\beta$  decay of  $^{137}\text{Xe}$ , several levels in  $^{137}\text{Cs}$  between 800 and 2100 keV have been reported. Of these, the only one which appears to correspond to a level excited with the  $(^3\text{He}, d)$  reaction is one at 2071 keV, the energy of which is in good agreement with that of the strong  $l = 2$ ,  $J = \frac{3}{2}^+$  transition we see at an excitation of 2.07 MeV. Our  $l_p = 0$  and  $l_p = 5$  states would not be directly populated via the  $\beta$  decay and are unlikely to be observed in the  $\gamma$  spectra. The levels deduced to lie at 849- and 982-keV excitations on the basis of the  $\gamma$ -ray data are not in good enough energy agreement with the broad peak at  $\sim 800$  keV mentioned earlier to convince us of a relationship, but this possibility cannot be ruled out. A direct-reaction study,  $(^3\text{He}, d)$  or  $(d, n)$ , with higher resolution would be useful in resolving this question.

### 3. $^{138}\text{Ba}(d, ^3\text{He})^{137}\text{Cs}$

The  $^{137}\text{Cs}$  level structure was also investigated by proton pickup from  $^{138}\text{Ba}$ . The only two levels that are discernably excited with consistency are the ground and first excited states. The ground-state transition is  $l_p = 4$  and the first-excited-state transition is  $l_p = 2$ , as is shown in Fig. 8. As outlined previously, the occurrence of only two strong

transitions is interpreted as indicating that only two orbits are appreciably occupied by the six active protons of the  $^{138}\text{Ba}$  ground state. It is from this premise that we deduce  $J^\pi = \frac{5}{2}^+$  for the first excited state, a point drawn upon in the prior discussion of the stripping transition to this same state. The strength of the pick-up transitions to these two levels indicate that they can be considered as single-hole states relative to  $^{138}\text{Ba}$ , as

well as single-particle states relative to  $^{136}\text{Xe}$ .

#### 4. $^{138}\text{Ba}(^3\text{He}, d)^{139}\text{La}$

The ground and first excited states of  $^{139}\text{La}$  are populated via proton stripping on  $^{138}\text{Ba}$  by  $l_p = 4$  and 2 transitions, respectively, as is shown in Fig. 9. Arguments similar to those made for  $^{137}\text{Cs}$  result in our assigning  $J^\pi = \frac{7}{2}^+$  and  $\frac{5}{2}^+$ , respectively, to these states. These are the  $1g_{7/2}$  and  $2d_{5/2}$  sin-

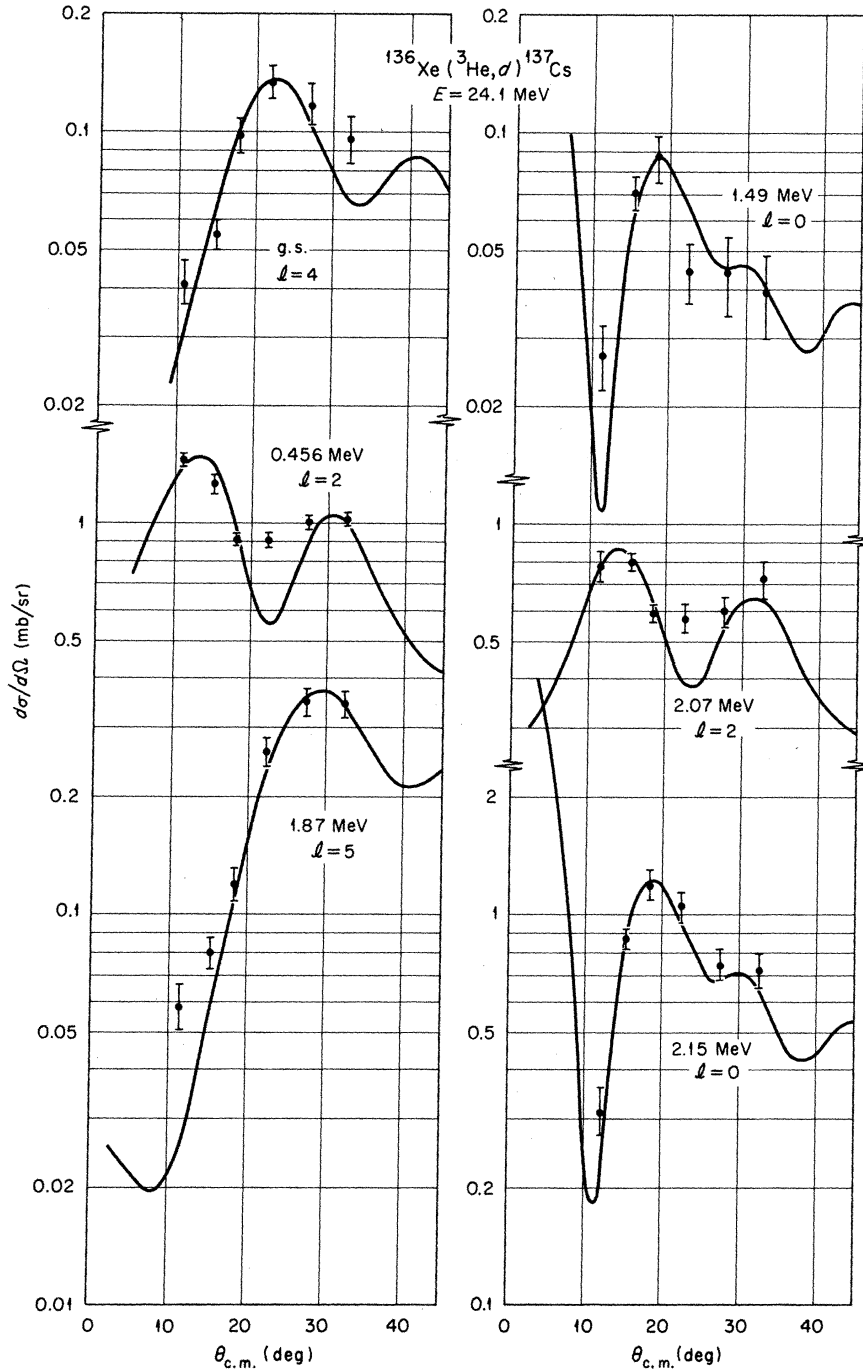


FIG. 7. Angular distributions of the observed transitions in the  $^{136}\text{Xe}(^3\text{He}, d)^{137}\text{Cs}$  reaction. The curves are DWBA predictions.

gle-particle states relative to  $^{138}\text{Ba}$ . No other states are seen (Fig. 3) up to an excitation of 1207 keV. Between 1200- and 2400-keV excitation, several levels are identified and their angular distributions measured. The data and DWBA curves are also shown in Fig. 9, and the results of the analysis listed in Table III. The  $l_p = 5$  ( $J^\pi = \frac{11}{2}^-$ ) state has moved down in excitation energy from its position

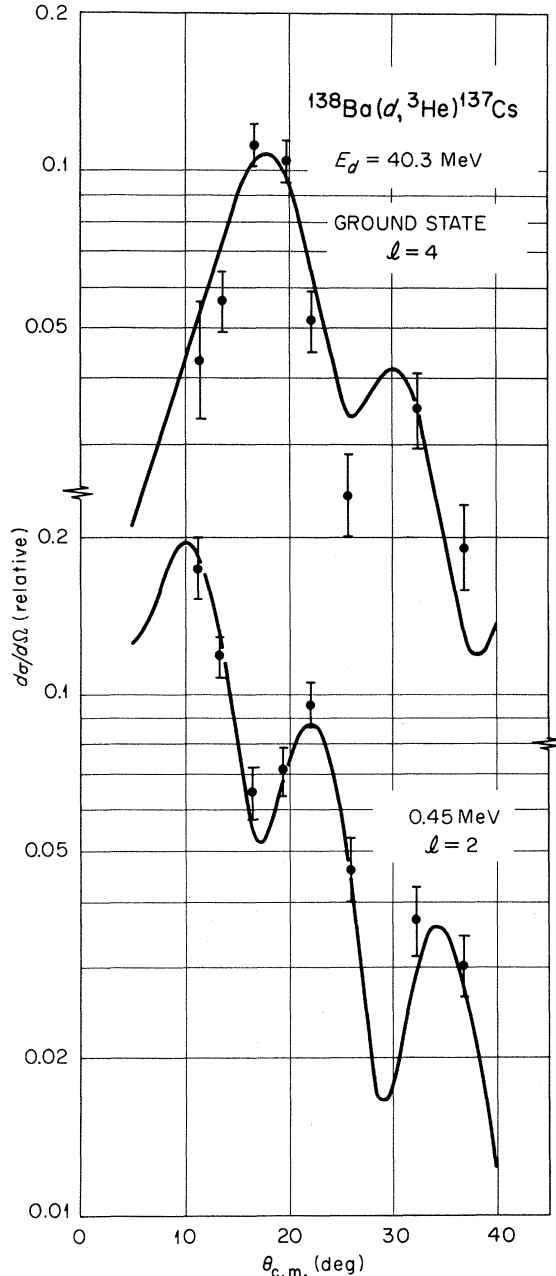


FIG. 8. Angular distributions of the transitions to the ground and first excited states of  $^{137}\text{Cs}$ , observed in the  $^{138}\text{Ba}(d, ^3\text{He})^{137}\text{Cs}$  reaction. The curves are DWBA predictions.

in  $^{137}\text{Cs}$ . The presence of several  $l_p = 0$  levels and several higher-lying  $l_p = 2$  levels indicates the partial fragmentation of the  $3s_{1/2}$  and  $2d_{3/2}$  single-particle states. The largest fragments of each lie at 1.78-MeV excitation and are not experimentally resolved in the spectra, a situation which creates an additional problem in extracting these important spectroscopic factors. It should be clearly noted that the employment of  $J^\pi = \frac{3}{2}^+$  for all of the higher  $l_p = 2$  transitions is an assumption of convenience only, since states with spectroscopic factors which are a small fraction of unity could be either  $\frac{5}{2}^+$  or  $\frac{3}{2}^+$ . Nonetheless, we tend to believe that they are all  $\frac{3}{2}^+$ .

In the interim since the first report of the ( $^3\text{He}, d$ ) results<sup>1</sup> several investigators<sup>23-27</sup> have published level schemes of  $^{139}\text{La}$  obtained either through observation of the  $\gamma$ -ray decay of levels populated by  $\beta$  decay or by inelastic scattering of neutrons or  $\gamma$  rays. The results of older studies of the  $^{139}\text{La}$  level structure are generally suspect since they typically report levels in the 200-1100-keV region of excitation energy, where the consensus of later studies indicates no states at all. It appears that all of the states seen via ( $^3\text{He}, d$ ) have been observed with one or more of the other experimental techniques. The high level density above 1400 keV makes an unambiguous rationalization of the various experimental results impractical for the present, however.

#### 5. $^{140}\text{Ce}(d, ^3\text{He})^{139}\text{La}$

The dominant pick-up transitions, (see Fig. 2) to  $^{139}\text{La}$  from  $^{140}\text{Ce}$  are to the ground state, with  $l_p = 4$ , and to the first excited state at 166 keV, with  $l_p = 2$ . These angular distributions are shown in Fig. 10. This leads to the assignments  $J^\pi = \frac{7}{2}^+$  and  $\frac{5}{2}^+$ , respectively, for these levels. They have  $1g_{7/2}$  and  $2d_{5/2}$  single-hole characters relative to  $^{140}\text{Ce}$ . A very weak transition can be detected to a level with energy corresponding to the level excited with  $l_p = 5$  in the  $^{139}\text{Ba}(^3\text{He}, d)^{139}\text{La}$  reaction. We assume that the state seen in pickup is the single-particle  $1h_{11/2}$  state and use the observed pickup intensity to set an upper limit for the occupation probability of  $1h_{11/2}$  in the ground state of  $^{140}\text{Ce}$ . The results are listed in Table III. The  $l = 0$  and  $l = 2$  spectroscopic factors which could be extracted from the small peak at 1.78 MeV are negligible.

#### 6. $^{140}\text{Ce}(^3\text{He}, d)^{141}\text{Pr}$

The ground state of  $^{141}\text{Pr}$  is populated in proton stripping with an  $l_p = 2$  transition, while an  $l_p = 4$  transition, which in the lighter nuclei is associated with the ground state, now populates the first

excited state at 145 keV. These two states are again associated with the addition of protons into the  $2d_{5/2}$  and  $1g_{7/2}$  orbits, respectively. This is consistent with the results of the  $(d, {}^3\text{He})$  reaction to  ${}^{141}\text{Pr}$  and with the previous<sup>5,6</sup> assignments of  $\frac{5}{2}^+$  and  $\frac{7}{2}^+$  to these levels based on atomic beam

and decay methods. The next state observed with the  $({}^3\text{He}, d)$  reaction lies at 1.11-MeV excitation and has an  $l_p = 5$  angular distribution. Levels at excitations of 1.30 and 1.65 MeV are populated with  $l_p = 0$  transitions and a level at 1.60 MeV is populated with  $l_p = 2$  transfer. Thus, making our

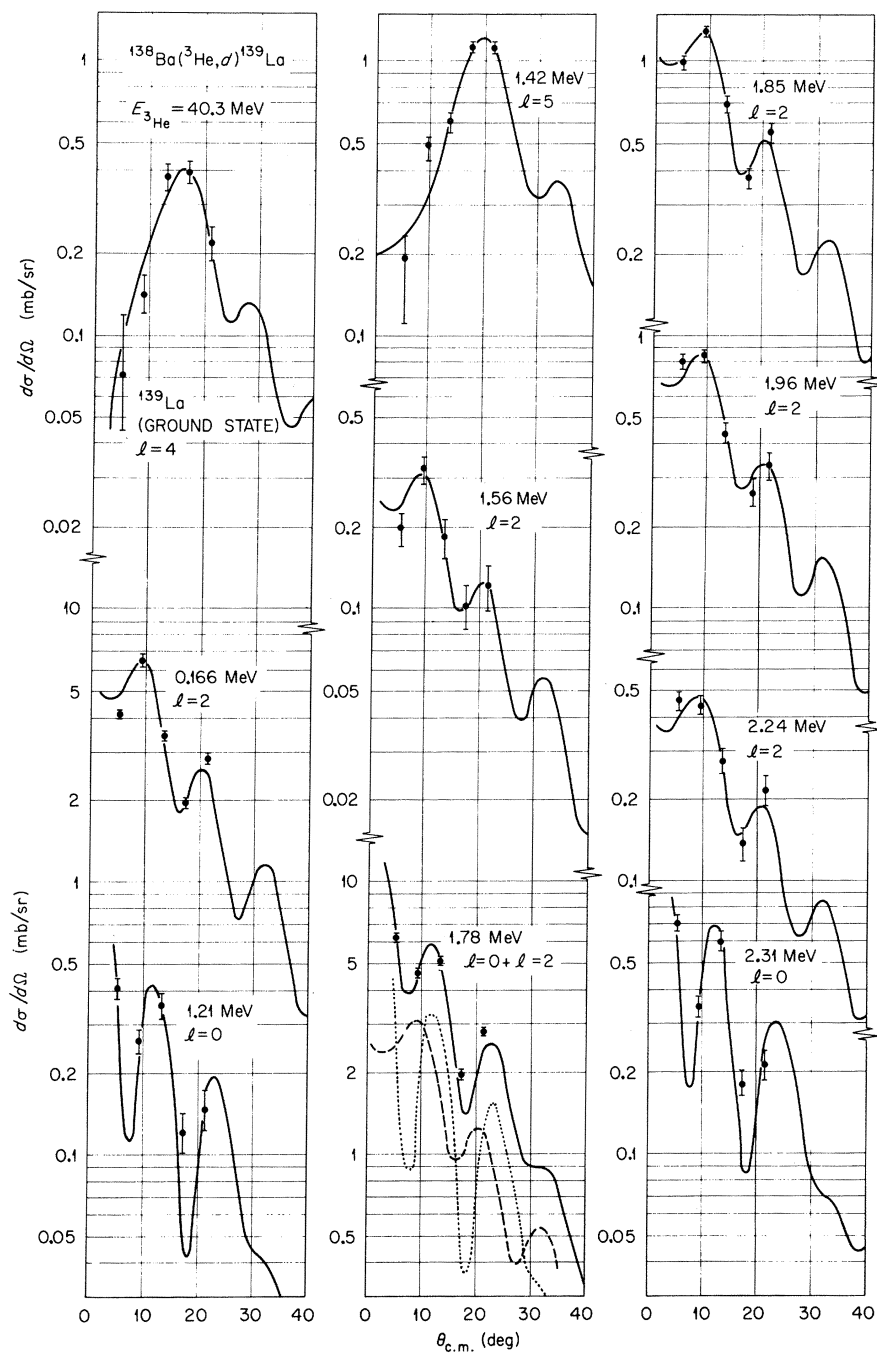


FIG. 9. Angular distributions of the observed transitions in the  ${}^{138}\text{Ba}({}^3\text{He}, d){}^{139}\text{La}$  reaction. The curves are DWBA predictions. The curve for the 1.78-MeV transition is a sum of  $l_p = 0$  and  $l_p = 2$  predictions.

usual assumption that strong stripping transitions to higher states represent population of the higher orbits of the  $gdhs$  shell, only one level each is observed for  $1h_{11/2}$  and  $2d_{3/2}$  while the  $3s_{1/2}$  strength is fairly evenly split between two levels. The angular distributions and DWBA curves are shown in Fig. 11.

As was the case for  $^{139}\text{La}$ , there have been numerous recent high-resolution studies of the  $^{141}\text{Pr}$  energy level spectrum in which  $\gamma$  decays are observed from levels excited by  $\beta^+$ -decay, inelastic

neutron, or  $\gamma$ -ray scattering.<sup>25-30</sup> In this instance it appears possible to make unambiguous correlations of the levels seen here with the consensus of level-energy assignments from the  $\gamma$ -ray data. The  $l_p = 5$  level at 1.11 MeV corresponds to the level seen in  $(n, n'\gamma)$  at 1.118 MeV. The  $l_p = 0$  level at 1.30 MeV corresponds to a level seen in both  $(\beta^+, \gamma)$  and  $(n, n'\gamma)$  at 1.299 MeV while the second  $\frac{1}{2}^+$  state at 1.65 MeV is listed at 1.650 MeV from  $(n, n'\gamma)$  and at 1.657 MeV from the  $(\beta^+, \gamma)$  work. The  $l_p = 2$  level at 1.60 MeV corresponds to the level seen at 1.607 MeV with both the  $(\beta^+, \gamma)$  and  $(n, n'\gamma)$  reactions. Numerous other states observed in the rather nonselective  $(n, n')$  reaction are not detectable in the  $(^3\text{He}, d)$  spectra, but this is to be expected.

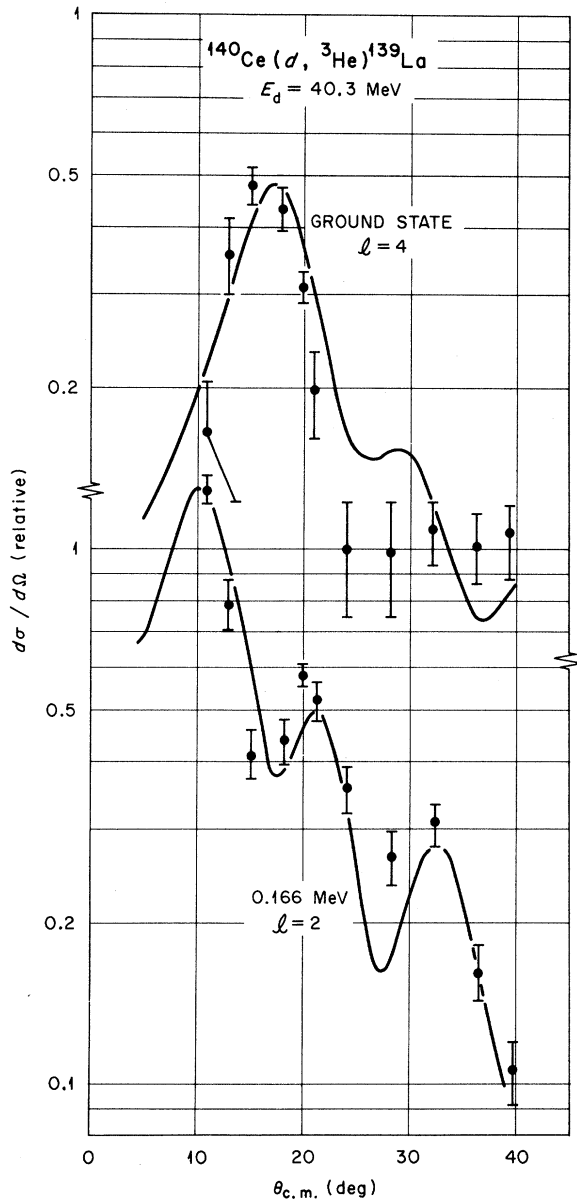


FIG. 10. Angular distributions of the transitions to the ground and first excited states of  $^{139}\text{La}$ , observed in the  $^{140}\text{Ce}(d, ^3\text{He})^{139}\text{La}$  reaction. The curves are DWBA predictions.

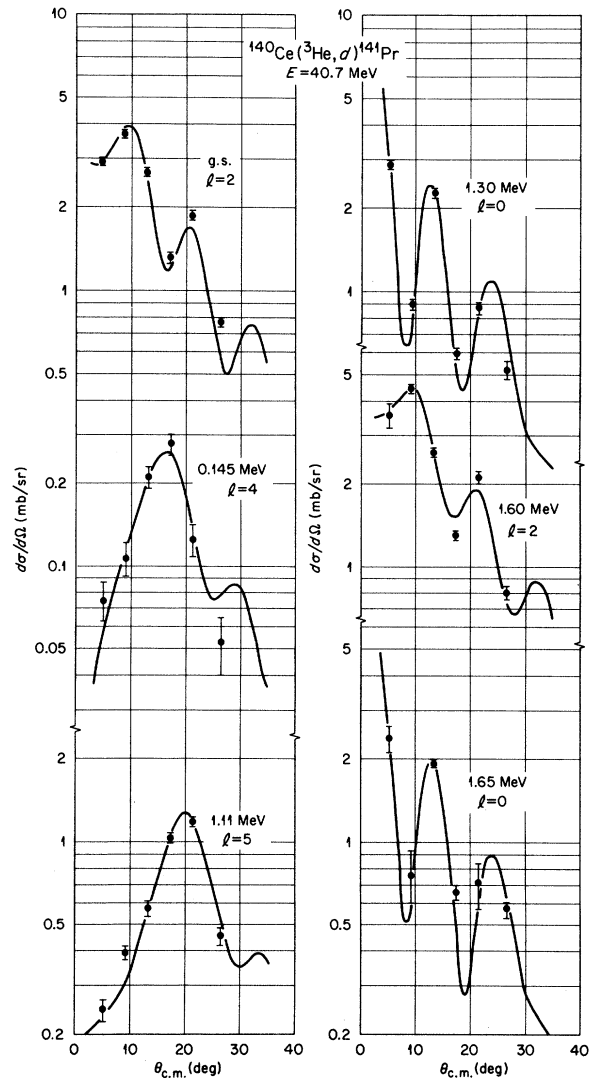


FIG. 11. Angular distributions of the transitions observed in the  $^{140}\text{Ce}(^3\text{He}, d)^{141}\text{Pr}$  reaction. The curves are DWBA predictions.

7.  $^{142}\text{Nd}(d, ^3\text{He})^{141}\text{Pr}$ 

The spectroscopic factors extracted from the  $l_p = 2$  and  $l_p = 4$  angular distributions (see Fig. 12) to, respectively, the ground and first excited states of  $^{141}\text{Pr}$  are large. Arguing as before, this leads to the inference of  $J = \frac{5}{2}^+$  and  $\frac{7}{2}^+$ , and  $2d_{5/2}$  and  $1g_{7/2}$  single-hole characters relative to  $^{142}\text{Nd}$ , for these levels.

There is evidence in the  $^3\text{He}$  spectra (see Fig. 2) for the population of levels at excitations of 1.11, 1.30, and 1.62 MeV, energies which correspond to the energies of the higher "gths" single-particle states observed with the  $(^3\text{He}, d)$  reaction to  $^{141}\text{Pr}$ . We assume the correspondence, even though the  $(d, ^3\text{He})$  data do not provide conclusive angular distributions for these levels. The small observed

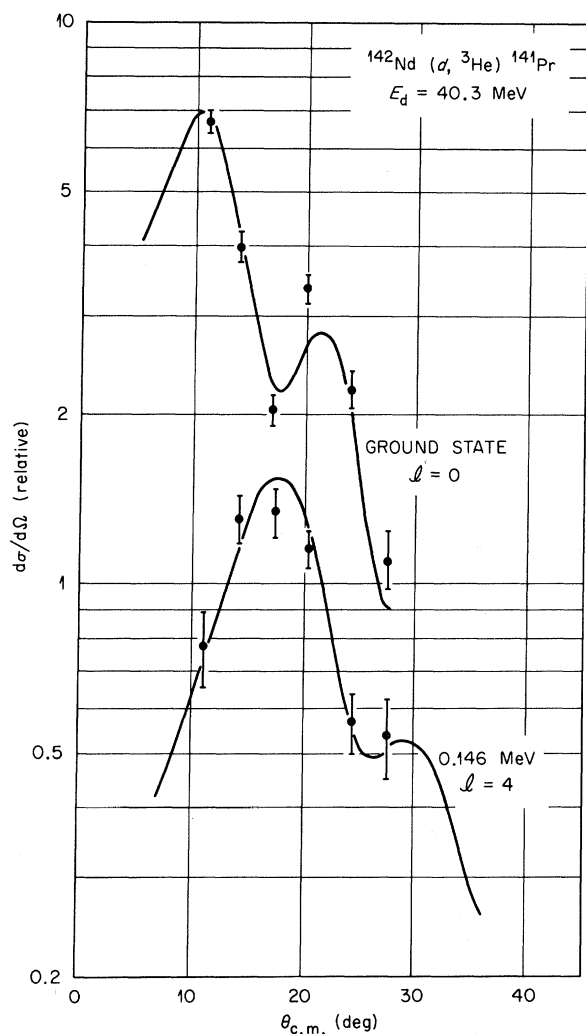


FIG. 12. Angular distributions of the transitions to the ground and first excited states of  $^{141}\text{Pr}$ , observed in the  $^{142}\text{Nd}(d, ^3\text{He})^{141}\text{Pr}$  reaction. The curves are DWBA predictions.

cross sections correspond to negligible spectroscopic strength for the  $3s_{1/2}$  and  $2d_{3/2}$  states but, as in the case of the  $^{140}\text{Ce}(d, ^3\text{He})^{139}\text{La}$  reaction, the upper limit on the  $1h_{11/2}$  spectroscopic factor is significant. Our conclusions are similar to those obtained by other workers with the same reaction.<sup>31</sup>

8.  $^{142}\text{Nd}(^3\text{He}, d)^{143}\text{Pm}$ 

The angular distributions to the levels of  $^{143}\text{Pm}$  noted in Fig. 3 are shown in Fig. 13. Comparing the levels of  $^{143}\text{Pm}$  to those of  $^{141}\text{Pr}$ , we find the following changes. There is a larger separation between the  $l_p = 4$  first-excited state and the  $l_p = 2$  ground state. The excitation energy of the  $1h_{11/2}$

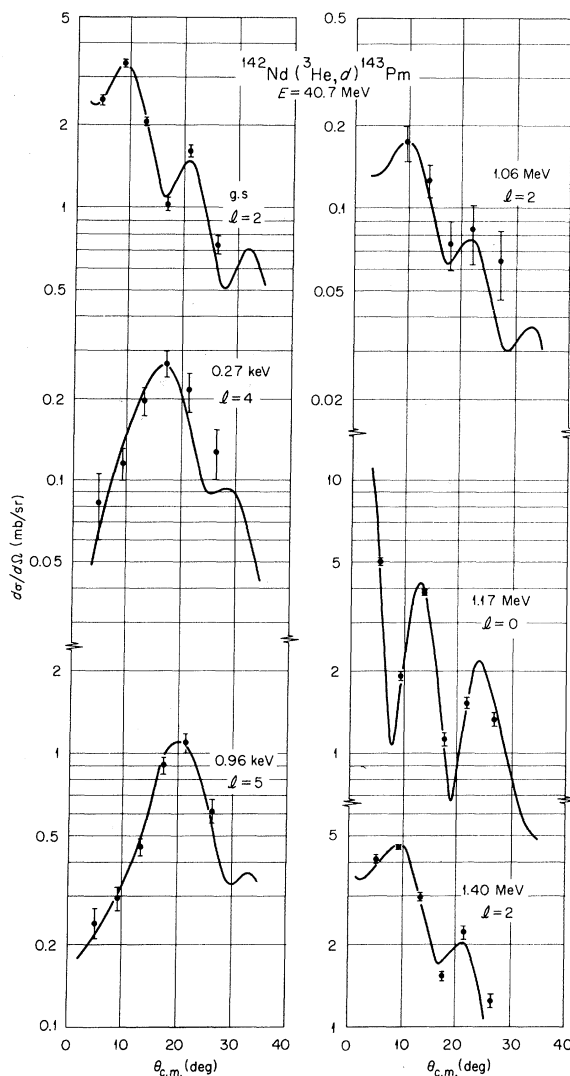


FIG. 13. Angular distributions of the transitions observed in the  $^{142}\text{Nd}(^3\text{He}, d)^{143}\text{Pm}$  reaction. The curves are DWBA predictions.

single-particle state has continued to decrease, and the  $l_p=0$ ,  $3s_{1/2}$ , strength is now concentrated in one, not two final states. Most of the  $l_p=2$ ,  $2d_{3/2}$ , strength is found in a state at 1.40-MeV excitation, but a weakly excited  $l_p=2$  state is also seen at 1.04 MeV.

The  $Q$  value for this reaction had a listed<sup>10</sup> uncertainty of 300 keV. From our data we deduced the new value listed in Table I.

### 9. $^{144}\text{Sm}(d, ^3\text{He})^{143}\text{Pm}$

The increasing occupation probabilities in  $^{144}\text{Sm}$  of the higher  $gdhs$  orbits made it feasible to obtain definitive  $(d, ^3\text{He})$  angular distributions, shown in Fig. 14, for the five states of  $^{143}\text{Pm}$  excited with significant strength in  $(^3\text{He}, d)$  reaction. The  $(d, ^3\text{He})$  results are consistent with the conclusions drawn from the  $(^3\text{He}, d)$  data. Proton pickup has also been studied on  $^{144}\text{Sm}$  by the  $(t, \alpha)$  reaction<sup>32</sup> at 13-MeV bombarding energy. Although in that study the resulting angular distributions were not distinctive enough to permit definite  $l_p$  assignments to be made, the correct assumptions were made in each case, and the resulting spectroscop-

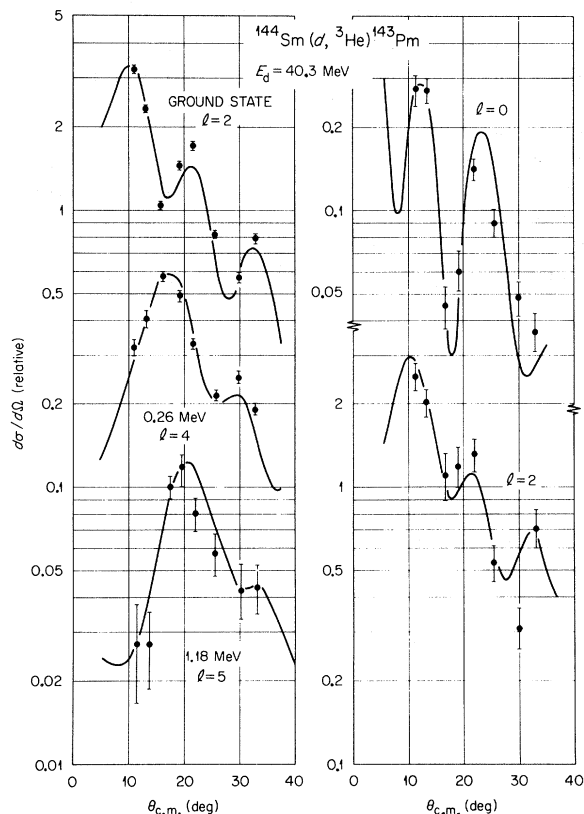


FIG. 14. Angular distributions of the transitions observed in the  $^{144}\text{Sm}(d, ^3\text{He})^{143}\text{Pm}$  reaction. The curves are DWBA predictions.

ic factors extracted for the various transitions are in reasonable agreement with those of Table III. In addition to the five transitions seen in  $(d, ^3\text{He})$ , the  $(t, \alpha)$  reaction also excited levels tentatively at 1.58 and 1.64 MeV and definitely at 1.85 and 1.97 MeV.

The information gained about the  $^{143}\text{Pm}$  energy level spectrum from the proton transfer reactions can be compared to the results of a study<sup>33</sup> of the decay of  $^{143}\text{Sm}$ . In this study, levels in  $^{143}\text{Pm}$  are found at 0.273, 1.057, 1.173, 1.341, 1.404, 1.516, 1.751, and 1.817 MeV. Of these, those at 1.057, 1.173, and 1.404 MeV should correspond to the  $l_p=2$ , 0, and 2 states, respectively, seen in proton transfer at essentially the same energies. The conclusions drawn about the level structure of  $^{143}\text{Pm}$  on the basis of the decay work are in serious disagreement with the proton-transfer results, however. These conclusions were that the 1.057-MeV level was the  $3s_{1/2}$  single-particle state and that the 1.516-MeV level was the  $2d_{3/2}$  single-particle state. Furthermore, the three levels lying

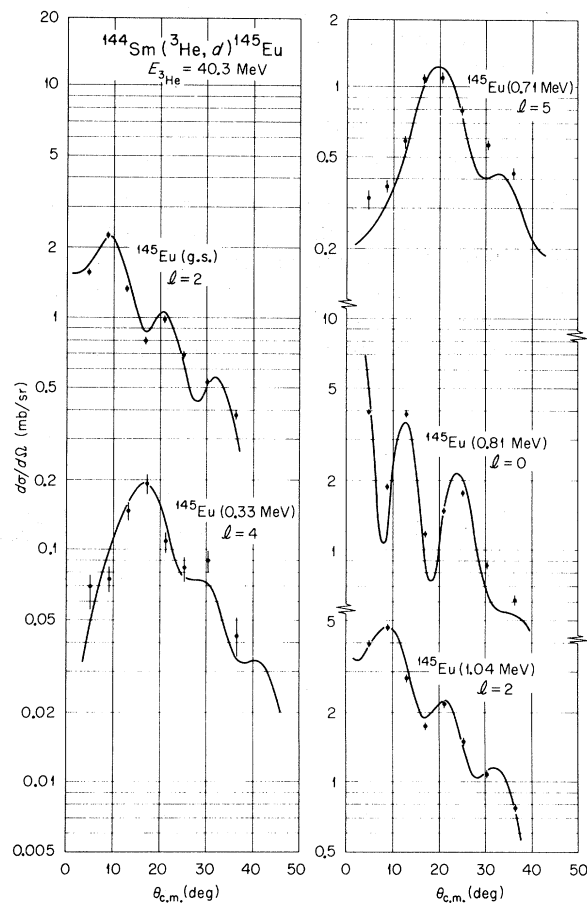


FIG. 15. Angular distributions of the transitions observed in the  $^{144}\text{Sm}(^3\text{He}, d)^{145}\text{Eu}$  reaction. The curves are DWBA predictions.

between these two were tentatively all assigned  $J = \frac{1}{2}$ . As mentioned, the stripping results indicated that the 1.057-MeV state is only weakly excited, and with an  $l_p = 2$  transfer which rules out  $J = \frac{1}{2}$ . The  $3s_{1/2}$  single-particle state corresponds, rather, to the level at 1.173 MeV. Finally, the  $2d_{3/2}$  state is the level seen at 1.404 MeV, not the one at 1.516 MeV, since the former is populated strongly with an  $l_p = 2$  ( ${}^3\text{He}, d$ ) transition while the latter is not measurably excited.

#### 10. ${}^{144}\text{Sm}({}^3\text{He}, d){}^{145}\text{Eu}$

The  ${}^{144}\text{Sm}({}^3\text{He}, d){}^{145}\text{Eu}$  reaction populates the ground state of  ${}^{145}\text{Eu}$  with an  $l_p = 2$  transition and populates excited states at 0.33-, 0.713-, 0.809- and 1.042-MeV excitation energies with transitions of  $l_p = 4, 5, 0,$  and  $2,$  respectively. The angular distributions and DWBA curves are presented in Fig. 15. These levels are taken to correspond to the coupling of  $2d_{5/2}, 1g_{7/2}, 1h_{11/2}, 3s_{1/2},$  and  $2d_{3/2}$  protons to a core consisting of the  ${}^{144}\text{Sm}$  ground state. The characteristics of these states are consistent with the trends established for the five *gdhs* single-particle states in the lighter nuclei. Detailed discussion of the  ${}^{145}\text{Eu}$  results have been presented elsewhere.<sup>3</sup>

### C. Commentary

#### 1. Energy Centroids of *gdhs* Orbits

The ( ${}^3\text{He}, d$ ) results provide a means of locating the energy centroids of the  $1h_{11/2}, 3s_{1/2},$  and  $2d_{3/2}$  proton orbits. In every target studied the total observed  $l_p = 5$  strength is found concentrated into a single final state. The  $2d_{3/2}$  and  $3s_{1/2}$  strengths are essentially concentrated into one state each

for the lightest and heaviest nuclei studied, but in  ${}^{141}\text{Pr}$  and  ${}^{139}\text{La}$  significant fragmentation is observed. Only one  $l_p = 4$  transition is observed for each target and we assume, with some justification, that only one  $2d_{5/2}$  state is populated.

The trends as a function of mass (or proton number) of the centroids of the higher three *gdhs* orbits relative to the low-lying  $\frac{7}{2}^+ - \frac{5}{2}^+$  doublets are displayed in Fig. 16. The trend lines are drawn through the centroids of the various orbits where several fragments exist. The length of the line corresponding to an observed energy level indicates the relative magnitude of its spectroscopic factor. We see that as protons are added in going from  ${}^{137}\text{Cs}$  to  ${}^{145}\text{Eu}$  [both the ( $d, {}^3\text{He}$ ) and ( ${}^3\text{He}, d$ ) results indicate that the added protons are filling the  $1g_{7/2}$  and  $2d_{5/2}$  orbits predominantly] the excitation energies of the  $1h_{11/2}, 3s_{1/2},$  and  $2d_{3/2}$  states decrease smoothly. At the same time their energies relative to each other remain essentially constant.

#### 2. Evaluation of Differences Between the Standard and Modified DWBA Analyses

The results of the present measurements can be used to test the efficacy of the modified form of the standard DWBA analysis of transition intensities, outlined in a previous section, in which the radius of the spin-orbit term of the bound-state well is reduced by 10% relative to the radius of the central well.

If the normalization of the stripping results for a given target is assigned so as to satisfy the overall sum rule for the entire *gdhs* shell, then consistency demands that the sum rules for all individual orbits must be satisfied simultaneously.

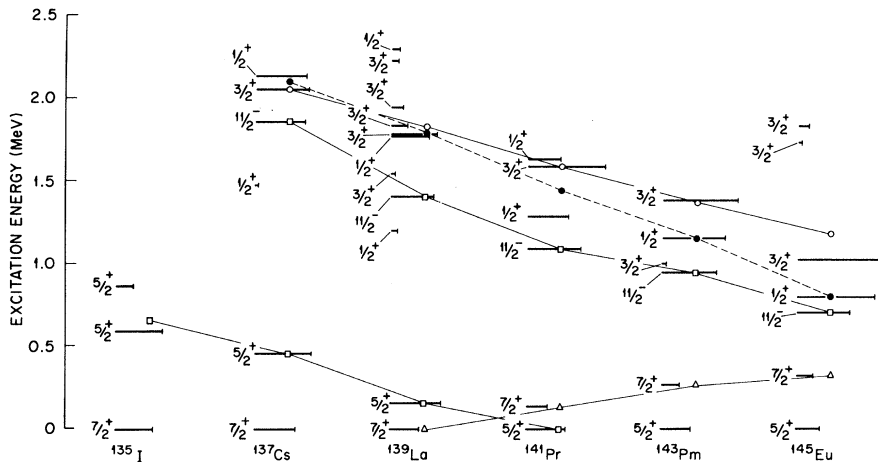


FIG. 16. Synopsis of ( ${}^3\text{He}, d$ ) results. All levels observed in the stripping studies are indicated. The excitation energies are noted by vertical positioning and the magnitudes of the spectroscopic factors indicated by the extent of the horizontal lines marking each level. The sloping lines trace the movements of the centroids of the various *gdhs* orbits. The pickup results to  ${}^{135}\text{I}$  are included in analogous fashion to the stripping results.

Thus, the sum of stripping spectroscopic factors for a particular  $J$  value in a given reaction must be less than or equal to 1.0. Violations of these limits are a measure of the internal inconsistencies in the way in which the DWBA analysis distributes the spectroscopic strength among the various transitions. This assumes of course, accurate experimental data and the proper normalization of the DWBA predictions to the experimental points.

Inspection of the numbers in Table III shows that for the transitions to  $^{139}\text{La}$ ,  $^{141}\text{Pr}$ ,  $^{143}\text{Pm}$ , and  $^{145}\text{Eu}$  the sum-rule limits on the  $2d_{3/2}$  transitions are violated to the extent of 25 to 35% in the standard DWBA analysis, while the modified analysis yields violations only of the order of 10–20%. The possibility that some of the higher  $l_p = 2$  transitions could correspond to the  $2d_{5/2}$  orbit rather than the  $2d_{3/2}$  does not significantly alter the conclusion to be drawn, since in most cases there is a single  $l_p = 2$  transition which by itself exceeds the limit on  $S(2, 2, \frac{3}{2})$ . In a similar fashion, it can be seen that the limits on the  $3s_{1/2}$  orbit are exceeded by about 15% in the standard analysis and to about half that in the modified results. We feel that dis-

crepancies of the order of 10% are to be expected from the uncertainties in the experimental statistics and curve-fitting procedures. Hence, the modified analysis appears to give relative value of the DWBA cross sections for different transferred orbital angular momenta which are consistent to within better than 10%.

A different kind of consistency check, also discussed in Sec. III, is available from a comparison of the pick-up and stripping results from the same target nucleus. The pick-up spectroscopic factors listed in Table III are in each case normalized so the sum of occupancy in the  $1g_{7/2}$  and  $2d_{5/2}$  orbits is equal to the occupancy implied for these two orbits by the analysis of the complementary stripping reaction. Thus, the occupation number for a particular orbit in a given target wave function should, ideally, be the same, whether extracted from the ( $d$ ,  $^3\text{He}$ ) or the ( $^3\text{He}$ ,  $d$ ) data. The actual values are listed in Table IV.

The comparison is most meaningful for the heavier nuclei. For  $^{140}\text{Ce}$ ,  $^{142}\text{Nd}$ , and  $^{144}\text{Sm}$ , an inspection of Table IV shows that the corresponding occupation numbers deduced from stripping and pick-up data with the modified analysis are

TABLE IV. Occupation probabilities  $\langle nlj \rangle$  for the proton orbits of the  $gdhs$  shell as obtained for the ground states of the even-mass  $N = 82$  nuclei from analysis of pick-up and stripping reactions.

Nucleus	Orbit	$\langle nlj \rangle$				Best values and estimated uncertainties
		Mod. DWBA		Stand. DWBA		
		( $^3\text{He}$ , $d$ )	( $d$ , $^3\text{He}$ )	( $^3\text{He}$ , $d$ )	( $d$ , $^3\text{He}$ )	
$^{136}\text{Xe}$	$1g_{7/2}$	3.2	2.7	2.0	1.8	$3.5 \pm 0.4$
	$2d_{5/2}$	0	.4	.1	.2	$0.5 \pm 0.2$
	$2d_{3/2}$	0.7		0.3		$0.0 \pm 0.2$
	$3s_{1/2}$	0.1		0.1		$0.0 \pm 0.2$
	$1h_{11/2}$	0		1.6		$0.0 \pm 0.7$
$^{138}\text{Ba}$	$1g_{7/2}$	4.6	3.9	3.7	3.6	$4.3 \pm 0.4$
	$2d_{5/2}$	0.35	1.0	0.60	0.70	$0.7 \pm 0.3$
	$2d_{3/2}$	0		0		$0.0 \pm 0.2$
	$3s_{1/2}$	0.3		0.2		$0.0 \pm 0.2$
	$1h_{11/2}$	2.0		3.5		$1.0^{+0.9}_{-0.7}$
$^{140}\text{Ce}$	$1g_{7/2}$	5.8	6.2	5.2	6.1	$5.6 \pm 0.3$
	$2d_{5/2}$	2.2	1.7	2.2	1.3	$1.8 \pm 0.2$
	$2d_{3/2}$	0		0		$0.0 \pm 0.2$
	$3s_{1/2}$	0		0		$0.0 \pm 0.2$
	$1h_{11/2}$	0.5	0.7	2.0	0.6	$0.6^{+0.6}_{-0.5}$
$^{142}\text{Nd}$	$1g_{7/2}$	6.0	6.1	5.4	6.2	$5.7^{+0.2}_{-0.4}$
	$2d_{5/2}$	2.8	2.7	2.9	2.1	$2.6^{+0.2}_{-0.3}$
	$2d_{3/2}$	0	0	0	0	$0.2 \pm 0.1$
	$3s_{1/2}$	0	0.1	0	0.1	$0.2 \pm 0.1$
	$1h_{11/2}$	2.1	1.0	3.5	0.9	$1.3^{+0.6}_{-0.4}$
$^{144}\text{Sm}$	$1g_{7/2}$	6.6	6.8	6.2	7.5	$6.3 \pm 0.2$
	$2d_{5/2}$	4.0	3.8	4.0	3.2	$3.6^{+0.1}_{-0.2}$
	$2d_{3/2}$	0	0.5	0	0.5	$0.3 \pm 0.1$
	$3s_{1/2}$	0	0.2	0	0.2	$0.2 \pm 0.1$
	$1h_{11/2}$	2.0	1.6	3.3	1.4	$1.6 \pm 0.3$

clearly more consistent with each other than are those obtained with the standard analysis. For  $^{138}\text{Ba}$  and  $^{136}\text{Xe}$ , the conclusions are mixed. If only the  $1g_{7/2}$  and  $2d_{5/2}$  orbits are considered, then the "modified" results are less consistent than the "standard" results, but, if the  $1h_{11/2}$  state is considered, then the "modified" values are in better agreement. We feel that the major problem here is that the small occupancy of the  $2d_{5/2}$  orbit in the lightest targets, leading as it does to stripping  $S$  factors near to 1.0, make the occupation numbers extracted from stripping too sensitive to uncertainties of the order of 5% in the  $S$  factor, as was explained in Sec. III C.

Hence, we conclude in these examples also that the modified analysis leads to results which are internally more consistent than those which are obtained with the standard analysis. We will, accordingly, use the results of the modified analysis in the remaining discussion.

### 3. Configurations of Ground-State Wave Functions

(a)  $^{136}\text{Xe}$ . The ( $^3\text{He}, d$ ) data indicate some vacancy for the  $2d_{3/2}$  orbit in the ground state of  $^{136}\text{Xe}$ . This is inconsistent with the conclusions drawn from the ( $^3\text{He}, d$ ) data on the other nuclei and we believe that it is spurious, resulting from the failure to identify, detect, or correctly extract the remaining  $2d_{3/2}$ ,  $l_p = 2$  strength. The relatively low quality of the  $^{136}\text{Xe}(^3\text{He}, d)^{137}\text{Cs}$  spectra is consistent with the possibility that such strength could have been missed. There is no evidence in the stripping results for the occupancy of the  $1h_{11/2}$  or  $3s_{1/2}$  orbits and we conclude that, to the limit of the accuracy of the present study, the active protons in the wave function of the  $^{136}\text{Xe}$  ground state occupy only the  $1g_{7/2}$  and  $2d_{5/2}$  orbits. From the pickup results on  $^{136}\text{Xe}$ , we recall that two  $l_p = 2$  levels in  $^{135}\text{I}$  were excited with comparable strength, as opposed to only one in the heavier nuclei. This might be taken as evidence for significant occupation of the  $2d_{3/2}$  orbit in  $^{136}\text{Xe}$ , something just ruled out in rather *ad hoc* fashion. However, the energy of the second  $l_p = 2$  level seen in  $^{135}\text{I}$  is significantly below the empirically extrapolated energy of the " $2d_{3/2}$ "  $\frac{3}{2}^+$  state in  $^{135}\text{I}$ . We believe that both of the  $^{135}\text{I}$  levels excited with  $l_p = 2$  are  $J^\pi = \frac{5}{2}^+$  and that the pick-up strength is shared between them by virtue of the convergence of the excitation energy of the  $2d_{5/2}$  single-particle state and the pairing energy.<sup>8</sup> The ratio of occupancy of  $1g_{7/2}$  protons to  $2d_{5/2}$  protons is taken from the ( $d, ^3\text{He}$ ) results. The value is 85%  $1g_{7/2}$  to 15%  $2d_{5/2}$ , or  $\langle 1g_{7/2} \rangle = 3.5 \pm 0.4$ ,  $\langle 2d_{5/2} \rangle = 0.5 \pm 0.2$ .

(b)  $^{138}\text{Ba}$ . The ( $^3\text{He}, d$ ) results indicate small occupancy of both the  $1h_{11/2}$  and  $3s_{1/2}$  orbits mixed

into the dominant  $1g_{7/2}$  and  $2d_{5/2}$  structure of the  $^{138}\text{Ba}$  ground state. The ( $d, ^3\text{He}$ ) data do not provide a check upon these  $1h_{11/2}$  and  $3s_{1/2}$  values. The  $3s_{1/2}$  value from stripping is not regarded as significant because of the difficulty in extracting the  $S$  factor from the  $l = 0 - l = 2$  doublet at 1.78 MeV in  $^{139}\text{La}$ . The occupation numbers we would choose for  $^{138}\text{Ba}$  are  $\langle 1g_{7/2} \rangle = 4.3 \pm 0.4$ ,  $\langle 2d_{5/2} \rangle = 0.7 \pm 0.3$ , and  $\langle 1h_{11/2} \rangle = 1.0_{-0.7}^{+1.0}$ .

(c)  $^{140}\text{Ce}$ . The results of the modified DWBA analysis of the ( $d, ^3\text{He}$ ) and ( $^3\text{He}, d$ ) data for  $^{140}\text{Ce}$  are in good agreement with each other. The following occupation values follow directly from the analysis:  $\langle 1g_{7/2} \rangle = 5.6 \pm 0.3$ ,  $\langle 2d_{5/2} \rangle = 1.8 \pm 0.2$ ,  $\langle 1h_{11/2} \rangle = 0.6_{-0.2}^{+0.6}$ , and  $\langle 3s_{1/2} \rangle$  and  $\langle 2d_{3/2} \rangle \leq 0.2$ .

(d)  $^{142}\text{Nd}$ . The "modified" spectroscopic factors from the ( $d, ^3\text{He}$ ) and ( $^3\text{He}, d$ ) experiments on  $^{142}\text{Nd}$ , when averaged and normalized, yield the following occupation numbers for the ground-state wave function:  $\langle 1g_{7/2} \rangle = 5.7_{-0.4}^{+0.2}$ ,  $\langle 2d_{5/2} \rangle = 2.6_{-0.3}^{+0.2}$ ,  $\langle 1h_{11/2} \rangle = 1.3_{-0.4}^{+0.6}$ , and  $\langle 3s_{1/2} \rangle$  and  $\langle 2d_{3/2} \rangle \leq 0.2$ . The increased lower limits on  $\langle 1g_{7/2} \rangle$  and  $\langle 2d_{5/2} \rangle$  reflect the uncertainty residing in undetermined occupancy of the  $2d_{3/2}$  and  $3s_{1/2}$  orbits.

(e)  $^{144}\text{Sm}$ . The ( $d, ^3\text{He}$ ) experiment on  $^{144}\text{Sm}$  yields unambiguous evidence for the occupancy of all of the *gdhs* orbits in the target ground state. Weighting these results with those from the ( $^3\text{He}, d$ ) reaction and normalizing to 12 particles produces the following values:  $\langle 1g_{7/2} \rangle = 6.3 \pm 0.2$ ,  $\langle 2d_{5/2} \rangle = 3.6 \pm 0.2$ ,  $\langle 1h_{11/2} \rangle = 1.6 \pm 0.3$ ,  $\langle 2d_{3/2} \rangle = 0.3 \pm 0.1$ , and  $\langle 3s_{1/2} \rangle = 0.2 \pm 0.1$ .

To summarize, there is reasonably precise evidence for the occupation of the  $2d_{3/2}$  and  $3s_{1/2}$  orbits only in the ground state of  $^{144}\text{Sm}$ , where, together, they account for a strength of about 0.5 particle. About half this much strength appears to occur in the  $^{142}\text{Nd}$  ground state and negligible amounts in the lighter nuclei.

In the case of the  $1h_{11/2}$  orbit, there is consistent evidence for about a 1.5-particle occupancy in the  $^{144}\text{Sm}$  and  $^{142}\text{Nd}$  ground states. This seems to decrease for  $^{140}\text{Ce}$  to about 0.5 particle but, with less conclusive evidence, to return to about 1.0 for  $^{138}\text{Ba}$ . There is no evidence for occupancy of this orbital in  $^{136}\text{Xe}$ . Our opinion is that the apparent decrease in occupation at  $^{140}\text{Ce}$  is real and the apparent increase in  $^{138}\text{Ba}$  is not, and that the "true" occupation of  $1h_{11/2}$  in  $^{138}\text{Ba}$  is probably close to 0.5 protons. The data for  $^{136}\text{Xe}$  are, of course, consistent with an occupation of  $1h_{11/2}$  of the order of 0.2–0.4 also. Thus, we estimate that the amount of filling of the  $1h_{11/2}$  orbit changes from something less than 5% in the four-particle system to a value of approximately 14% in the 12-particle system.

The occupancy of the  $2d_{5/2}$  orbital changes most

markedly in the progression from 4 to 12 active particles. In the ground state of  $^{136}\text{Xe}$ , this orbit is only 8% filled and this percentage increases rather smoothly to a value of 60% (3.6 particles out of a possible 6) in the ground state of  $^{144}\text{Sm}$ . The  $1g_{7/2}$  orbit is the most tightly bound member of the *gdhs* shell. To lowest order in the shell-model scheme it should fill (to eight particles) at  $^{140}\text{Ce}$ . Actually, we see that this orbit is only 70% filled in the ground state of  $^{140}\text{Ce}$  and, in fact, its percentage occupancy remains essentially fixed at 70% from  $^{140}\text{Ce}$  through  $^{144}\text{Sm}$ .

### V. SUMMARY

The experimental results we have presented constitute evidence for a close and systematic relationship between the eleven  $N = 82$  nuclei in the mass range  $A = 135$ – $145$ . Complementary pickup and stripping reactions on the ground states of each of the even-mass nuclei indicate that the protons outside the  $Z = 50$ ,  $N = 82$  core of these systems occupy the  $1g_{7/2}$  and  $2d_{5/2}$  orbits, predominantly, with the occupation of the  $1h_{11/2}$  orbit becoming appreciable towards  $A = 144$ .

Both the stripping and pickup reactions populate the lowest two levels in the odd-mass spectra, one level with  $l_p = 4$  and one with  $l_p = 2$ . The transitions are interpreted to involve transfer of  $1g_{7/2}$  and  $2d_{5/2}$  protons, respectively, and the spectroscopic factors are such as to indicate that the wave functions of these levels can be accurately approximated either as single particles coupled to the ground states of the stripping targets or as single holes coupled to the ground states of the pickup targets. Only one  $l_p = 4$  transition is observed in each different reaction, and only in the  $^{136}\text{Xe}(d, ^3\text{He})$ - $^{135}\text{I}$  reaction is there probable evidence for more than one  $2d_{5/2}$  transition. With this exception, the single-particle (hole) strengths for these two orbits are always concentrated into single levels.

A similar situation is observed for the single-particle strength of the  $1h_{11/2}$  orbit. Only one  $l_p = 5$  transition is observed in each stripping reaction. The  $1h_{11/2}$  single-particle states located in the stripping experiments are weakly populated via pickup from the heavier targets. The evidence is that this orbit is not significantly occupied relative to its capacity in any of the target wave functions.

The single-particle strengths of the  $2d_{3/2}$  and  $3s_{1/2}$  orbits are observed, in general, to be fragmented over several states each. The fragmentation is most significant for the  $^{139}\text{La}$  and  $^{141}\text{Pr}$  nuclei, but even in these cases the total strength is well concentrated and the "single-particle" levels can typically be identified without ambiguity.

The large-scale aspects of the structure of these

nuclear systems that the present experiments delineate are the apparent validity of the hypothesis of a  $Z = 50$ ,  $N = 82$  shell closure, the trends of the occupation probabilities of the five *gdhs* proton orbits as a function of proton number, and the energy orderings of the five *gdhs* "single-particle states," again as a function of mass. The finer details revealed include the quantitative ratios of occupation probabilities for the *gdhs* orbits, the quantum numbers and exact energies of the various observed levels, and the patterns of fragmentation of the single-particle strengths over these levels.

The comprehensive view of the  $N = 82$  nuclei that is developed is one of consistent simplicity in terms of the shell model. The dominant features of the odd-mass level structures can be discussed in terms of a proton in one of the five *gdhs* orbits coupled to core consisting of closed shells of 82 neutrons and 50 protons plus  $(Z - 50)$  protons paired off in the  $1g_{7/2}$  and  $2d_{5/2}$  orbits. The deviations in detail from this simple picture which appear also seem uniformly to be explicable in terms of *gdhs* shell configurations. Thus it seems reasonable to hope that structure calculations which explicitly consider only protons in the *gdhs* orbits can account for the phenomena we have observed in the present experiments in a complete and unified way. Indeed, the ability of present theoretical techniques to explain these regular and, relatively speaking, transparent aspects of the structure of the  $N = 82$  nuclei is a prerequisite if the same procedures are to reliably interpret the more complex phenomena observed in nuclei which lie off the shell closure. The extensive body of experimental information that is now available about the  $N = 82$  band of nuclei should make possible definitive evaluations of the various theoretical approaches to nuclear structure in this region.

### ACKNOWLEDGMENTS

We are grateful to Jerry Nolan and Bill Horath for their essential assistance in fabricating the Ba, Ce, and Nd targets. Two of the authors (BHW and RLA) were supported by U. S. Atomic Energy Commission Postdoctoral Fellowships, administered by Oak Ridge Associated Universities, during the period when part of the work reported here was carried out. Some other aspects of the project were accomplished while one author (BHW) was in residence at the Cyclotron Institute, Texas A & M University, College Station, Texas.

\*Work supported in part by the U. S. Atomic Energy Commission under contract with the Union Carbide Corporation.

†Present address: Cyclotron Laboratory, Michigan State University, East Lansing, Michigan 48823.

‡Work supported in part by the National Science Foundation.

<sup>1</sup>B. H. Wildenthal, E. Newman, and R. L. Auble, *Phys. Letters* **27B**, 628 (1968).

<sup>2</sup>E. Newman, R. L. Auble, and B. H. Wildenthal, *Bull. Am. Phys. Soc.* **13**, 70, 658 (1968); **14**, 56 (1969); B. H. Wildenthal, R. L. Auble, and E. Newman, *Bull. Am. Phys. Soc.* **13**, 1430 (1968); **14**, 1239 (1969).

<sup>3</sup>E. Newman, K. S. Toth, R. L. Auble, R. M. Gaedke, M. F. Roche, and B. H. Wildenthal, *Phys. Rev. C* **1**, 1118 (1970).

<sup>4</sup>M. G. Mayer and J. H. D. Jensen, *Elementary Theory of Nuclear Shell Structure* (John Wiley & Sons, Inc., New York, 1955).

<sup>5</sup>*Nuclear Data Sheets*, compiled by K. Way *et al.* (Printing and Publishing Office, National Academy of Sciences - National Research Council, Washington, D.C.).

<sup>6</sup>C. M. Lederer, J. M. Hollander, and I. Perlman, *Table of Isotopes* (John Wiley & Sons, Inc., New York, 1968), 6th ed.

<sup>7</sup>B. H. Wildenthal, *Phys. Rev. Letters* **22**, 1118 (1969) and *Phys. Letters* **29B**, 274 (1969).

<sup>8</sup>B. H. Wildenthal, E. Newman, and J. B. McGrory, to be published.

<sup>9</sup>The enriched samples of <sup>138</sup>Ba, <sup>140</sup>Ce, <sup>142</sup>Nd, and <sup>144</sup>Sm were obtained from the Isotopes Division of Oak Ridge National Laboratory. The sample of <sup>136</sup>Xe was obtained from Mound Laboratories.

<sup>10</sup>J. H. E. Mattauch, W. Thiele, and A. H. Wapstra, *Nucl. Phys.* **67**, 1 (1965).

<sup>11</sup>C. M. Jones and M. Mancusi, private communication.

<sup>12</sup>R. H. Bassel, R. M. Drisko, and G. R. Satchler, Oak Ridge National Laboratory Report No. ORNL-3240 (unpublished).

<sup>13</sup>E. Newman, L. C. Becker, B. M. Preedom, and J. C. Hiebert, *Nucl. Phys.* **A100**, 225 (1967).

<sup>14</sup>E. F. Gibson, B. W. Ridley, J. J. Kraushaar, M. E. Rickey, and R. H. Bassel, *Phys. Rev.* **155**, 1194 (1967).

<sup>15</sup>B. M. Preedom, E. Newman, and J. C. Hiebert, *Phys. Rev.* **166**, 1156 (1968).

<sup>16</sup>R. H. Bassel, *Phys. Rev.* **149**, 791 (1966).

<sup>17</sup>M. Dost and W. R. Herring, *Phys. Letters* **19**, 488 (1965).

<sup>18</sup>B. H. Wildenthal, B. M. Preedom, E. Newman, and M. R. Cates, *Phys. Rev. Letters* **19**, 960 (1967).

<sup>19</sup>E. Newman and B. H. Wildenthal, *Bull. Am. Phys. Soc.* **13**, 1436 (1968); W. C. Parkinson, D. L. Hendrie, H. H. Duhm, J. Mahoney, J. Saudinos, and G. R. Satchler, *Phys. Rev.* **178**, 1976 (1969).

<sup>20</sup>M. P. Fricke, E. E. Gross, B. J. Morton, and A. Zucker, *Phys. Rev.* **156**, 1207 (1967); G. W. Greenlees and G. J. Pyle, *ibid.* **149**, 836 (1966).

<sup>21</sup>M. H. Macfarlane and J. B. French, *Rev. Mod. Phys.* **32**, 567 (1960).

<sup>22</sup>G. Holm, *Arkiv Fysik* **37**, 1 (1967).

<sup>23</sup>J. C. Hill and M. L. Wiedenbeck, *Nucl. Phys.* **A119**, 53 (1968).

<sup>24</sup>G. Berzins, M. E. Bunker, and J. W. Starner, *Nucl. Phys.* **A128**, 294 (1969).

<sup>25</sup>J. G. Malan, W. R. McMurray, P. van der Merwe, I. J. van Heerden, and C. A. Engelbrecht, *Nucl. Phys.* **A124**, 111 (1969).

<sup>26</sup>P. van der Merwe, I. J. van Heerden, W. R. McMurray, and J. G. Malan, *Nucl. Phys.* **A124**, 433 (1969).

<sup>27</sup>R. Moreh, private communication.

<sup>28</sup>R. Moreh and A. Nof, *Phys. Rev.* **178**, 1961 (1969).

<sup>29</sup>D. B. Beery, W. H. Kelly, and W. C. McHarris, *Phys. Rev.* **171**, 1283 (1968).

<sup>30</sup>V. R. Dave, J. A. Nelson, and R. M. Wilenzick, *Nucl. Phys.* **A142**, 619 (1970).

<sup>31</sup>H. W. Baer and J. Bardwick, *Nucl. Phys.* **A129**, 1 (1969).

<sup>32</sup>O. Hansen, O. Nathan, L. Vistisen, and R. Chapman, *Nucl. Phys.* **A113**, 75 (1968).

<sup>33</sup>D. DeFrenne, K. Heyde, L. Dorikens-Vanpret, M. Dorikens, and J. Demuyneck, *Nucl. Phys.* **A110**, 273 (1968).

## Magnetic Dipole Moments of $p_{1/2}$ -Shell Nuclei

S. T. Hsieh

*Department of Physics, National Tsing Hua University, Hsinchu, Taiwan, China*

(Received 10 November 1970)

The magnetic dipole moments of  $p_{1/2}$ -shell nuclei are calculated by the first-order perturbation theory. It is shown that the tensor force which causes the configuration mixing is important to explain observed data of these moments.

The magnetic dipole moments of odd-mass nuclei have been estimated with the  $j$ - $j$ -coupling shell model and are known as Schmidt values. The agreement between the shell-model values and the

experimental values is not satisfactory. Also, most of the observed data lie within the regions bounded by the Schmidt lines instead of being scattered on both sides. Noya, Arima, and Horie<sup>1</sup>